Detailed Experimental Investigation for Foamed Bitumen Stabilisation

Transfund New Zealand Research Report No. 258

Detailed Experimental Investigation for Foamed Bitumen Stabilisation

M. Saleh, University of Canterbury
New Zealand

Transfund New Zealand Research Report No. 258

ISBN 0-478-25370-2
ISSN 1174-0574

PO Box 2331, Lambton Quay, Wellington, New Zealand
Telephone 64 4 473-0220; Facsimile: 64 4 499-0733

Saleh, M. 2004. Detailed experimental investigation for foamed bitumen stabilisation. *Transfund New Zealand Research Report No. 258.* 67 pp.

University of Canterbury, Private Bag 4800, Christchurch, New Zealand

Keywords: bitumen, CBR, cement, compaction water content, fatigue behaviour, foam, foam mixes, foamed bitumen, fracture energy, gradation curves, mixing water content, pavement, performance, resilient modulus, road, stabilisation, water content

An Important Note for the Reader

The research detailed in this report was commissioned by Transfund New Zealand. Transfund New Zealand is a Crown entity established under the Transit New Zealand Act 1989. Its principal objective is to allocate resources to achieve a safe and efficient roading system. Each year, Transfund New Zealand invests a portion of its funds on research that contributes to this objective.

While this report is believed to be correct at the time of its preparation, Transfund New Zealand, and its employees and agents involved in its preparation and publication, cannot accept any liability for its contents or for any consequences arising from its use. People using the contents of the document, whether directly or indirectly, should apply and rely on their own skill and judgement. If necessary, they should seek appropriate legal or other expert advice in relation to their own circumstances, and to the use of this report.

The material contained in this report is the output of research and should not be construed in any way as policy adopted by Transfund New Zealand but may form the basis of future policy.

Acknowledgments

Transfund New Zealand is thanked for its financial support which has made this research possible.

Also, I express my appreciation to the Department of Civil Engineering, University of Canterbury, in particular to Dr Andy Buchanan, Head of Department, who has provided an intellectually stimulating environment in which to work.

The contributions of the professional practitioners with whom I have worked have been invaluable. Some of the major contributors to this research include David Garner (Shell New Zealand), Nigel J Preston (Shell Australia), and Bruce Rule (Isaac Construction Ltd).

The contributions of Professor Michael Mamlouk (Arizona State University, USA) and Lloyd Houghton (Works Infrastructure) as peer reviewers were particularly valuable.

Contents

Abbreviations & Acronyms

γ_b	=	Bitumen density (assumed to be 1 g/cm^3)
ν	=	Poisson's ratio
$\tau_{1/2}$	=	Half-life time of foam (in seconds)
ER	=	Expansion ratio
ER_a	=	Actual expansion ratio
ER_m	=	Maximum measured expansion ratio
FI	=	Foam Index
G_{mb}	=	Bulk specific gravity of the compacted mix
G_b	=	Specific gravity of bitumen
G_{sb}	=	Bulk specific gravity of aggregates
G_{sa}	=	Apparent specific gravity of aggregates
HLT	=	Half-life time of foamed bitumen (in seconds)
IRS	=	Index of Retained Strength
ITS	=	Indirect tensile strength
OMC	=	Optimum moisture content of aggregates
MMC	=	Mixing moisture content
MFC	=	Mixing foam content
M_r	=	Resilient modulus
OMMC	=	Optimum mixing moisture content
OMFC	=	Optimum mixing foam content
P_b	=	Percent of bitumen by weight of total mix
PI	=	Penetration Index
PVN	=	Penetration-Viscosity Number
Q_w	=	Water flow rate (litres/hour)
Q_b	=	Bitumen flow rate (grams/second)
SSD	=	Saturated-Surface Dry condition
VTS	=	Viscosity-Temperature Susceptibility
V_b	=	Percent of bitumen by volume of the compacted mix
Wc	=	Percentage of foamant water

M20FA	=	Foam-stabilised mix with AP-20 aggregates and fly ash type C as mineral fillers
M20FA1C	=	Foam-stabilised mix with AP-20 aggregates and fly ash type C and 1.0% cement as mineral fillers
M20FA2C	=	Foam-stabilised mix with AP-20 aggregates and fly ash type C and 2.0% cement as mineral fillers
M20PA	=	Foam-stabilised mix with AP-20 aggregates and pond ash as mineral fillers
M20LM	=	Foam-stabilised mix with AP-20 aggregates and hydrated lime as mineral fillers
M40PA	=	Foam-stabilised mix with AP-40 aggregates and pond ash as mineral fillers
M40LM	=	Foam-stabilised mix with AP-40 aggregates and hydrated lime as mineral fillers

Executive Summary

Introduction

As the demand for a cost-effective and environmentally friendly pavement stabilisation method increases, so has foamed bitumen stabilisation for unbound granular pavement layers started to gain broad acceptance worldwide.

This report presents the second phase of the foamed bitumen stabilisation study which is to investigate the properties and the expected performance of the foamed bitumen-stabilised mixes, also called foam-stabilised mixes.

In the first phase[1], the research team investigated the feasibility of using foamed bitumen as a potential stabilising technique. Preliminary tests were carried out to evaluate the properties of the resulting foamed bitumen mixes.

For this second phase of the research, carried out in 2003-2004, a comprehensive testing programme has been conducted to inspect and characterise the behaviour of the foam-stabilised mixes. To make appropriate comparisons, nine bitumen types from seven different sources were examined for their rheological properties. The bitumens were selected from three sources (VEN, SHL, DLT) currently used in New Zealand, three sources (AR2000, AR4000-1, AR4000-2) in California, US, and one (C170) from Australia.

The rheological properties of the different sources of binders were studied to examine the relationship between the bitumen physical properties and the foamability characteristics of the resulting foam. The ability of the current system to characterise the quality of the foam was examined by comparing the different sources of foam, their properties, and their ability to effectively mix with aggregate particles.

Physical Properties of Bitumen

Consistency of bitumen (the degree of fluidity of bitumen at any particular temperature) is a major physical criterion in explaining bitumen rheological properties. Consistency tests involved in this investigation were penetration, viscosity and softening point. Both penetration and viscosity were carried out at different temperatures to investigate the temperature susceptibility of the different bitumens in order to explain the effects of bitumen rheological properties on the bitumen foaming characteristics and properties of the resulting mixes.

The temperature susceptibilities of the bitumen types were evaluated using three different approaches: Penetration Index (PI), Penetration-Viscosity Number (PVN), and Viscosity-Temperature Susceptibility (VTS).

Physical Properties of Bitumen Foams

Foamability tests were performed in which the percentage of foamant water was optimised. The expansion ratio (ER), half-life (HLT) and the foam index (FI) were used to determine the optimum foamant water content and to determine the quality of the foam. These parameters are the key indicators of the foam quality according to the current characterisation system. The FI combines the effect of both foam expansion and time of foam decay. It can be used to determine the optimum foamant water but sometimes the trend of FI against the percentage foamant water shows no peak. Therefore, the FI cannot provide the optimum foamant water content in such cases.

---

[1] Reported in Transfund New Zealand Research Report No. 250 (2003).

The VEN180 and AR4000-1 bitumens provided the best foam quality according to the current system of evaluation, while SHL80, DLT80 and C170 produced the lowest quality foams. Foams produced from SHL80, DLT80 and C170 were classified as unsuitable for foam stabilisation, and the foam produced from AR4000-2 was classified as poor.

With the exception of the C170 foam, all other foams regardless of their classification rank could be mixed effectively with aggregate. Because of the empirical nature of the measured parameters such as expansion ratio and half-life time, discrepancies between the classification of the foam and its actual quality were observed. Such inconsistencies in the current classification system have led to the proposal of a new system to characterise the quality of the foam, which was developed in this study.

The new system uses the Brookfield rotational viscometer to measure the viscosity of foam at different time intervals. The average foam viscosity over the first 60 seconds of foaming is used as a measure of the quality of the foam. This parameter is analogous to the foam index. Foam index combines both expansion ratio and time of decay of the foam, while Brookfield viscosity combines directly the foam viscosity and the first 60 seconds of foam decay. Because the viscosity of the foam is a fundamental property, this latter system is likely to provide a more reliable prediction of the quality of the foam regardless of its source. The foamant water content that provides the lowest average viscosity is considered the optimum foamant water content. Thus, the suggested new system of classification can avoid the discrepancies in the current characterisation system.

Foamed Bitumen Mix Design

Several mixes were prepared using different aggregate gradations (taken from midpoint of the AP-20 and the upper limit of AP-40) and different types of mineral fillers such as fly ash type C, Huntly pond ash, hydrated lime, and Portland cement. Huntly pond ash is a by-product of power generation boilers, and can cause an environmental hazard because of its alkalinity, high concentrations of boron, and presence of several heavy metals such as arsenic and cadmium. Using it in foam stabilisation was investigated as a potential safe way of discarding it economically. The optimum foam and water contents were determined so that the resilient modulus of the mixture is maximised. The optimum foam and water contents varied according to the aggregate gradation and the type of mineral fillers.

Volumetric Properties of Foam-stabilised Mixes

The specific gravities of the coarse and fine aggregates, and voids and density relationships of the compacted mix were evaluated.

The percentage of air voids in the total mix (%VA) was about twice that of the dense-graded HMA. Premature cracking and/or ravelling are likely to occur with air voids of the magnitude obtained for foam-stabilised mixes because of oxidation of bitumen, a consequence of which is reduction of pavement durability. The percentage of voids in the mineral aggregates (%VMA) is quite close to that of the HMA made with aggregate of similar maximum nominal size.

Mechanical Properties of Foam-stabilised Mixes

Temperature Susceptibility

Different foam-stabilised mixes were prepared at their optimum foam and water contents. As well bitumens from different sources were examined to identify the effect of their rheological properties on the foam-stabilised mixes. A dense graded AC10 hot mix asphalt (HMA) prepared by a local supplier was included in the tests for temperature susceptibility to provide a comparison with the foam-stabilised mixes.

The effects of both length of curing period, and testing temperature, on the resilient modulus values of foam-stabilised mixes were considerable. Higher temperature susceptibility was obtained as the specimens were subjected to longer curing times. It was also observed that specimens containing Portland cement had higher temperature susceptibility than those containing fly ash. This indicates that the type of mineral filler has an effect on the temperature susceptibility of the foam-stabilised mixes.

In correlation with the bitumen temperature susceptibility results, the PVN approach closely corresponds to the temperature susceptibility properties of foamed bitumen mixtures. VEN80 and VEN180 bitumen types were classified as yielding the least temperature-susceptible bitumens and produced the least temperature-susceptible mixes. The PVN approach, however, did not always detect the temperature susceptibility of all mixes. One example is AR-2000, which was classified as one of the most temperature-susceptible binders using the PVN approach, yielded mixtures that were not very temperature susceptible.

The resilient modulus of the HMA undergoes dramatic decrease at elevated temperatures, while the foam-stabilised mix still maintains relatively high resilient modulus values. This finding agrees with previous findings by other researchers. The high resilient modulus values of foam-stabilised mixtures at high temperatures can be attributed to the low binder content and the preservation of the friction between larger aggregate particles since they are not fully coated with binder (as in HMA). The high bitumen content of HMA makes it more temperature susceptible compared to foam-stabilised mixes. Therefore, foam-stabilised mixes are likely to suffer much less distortion and rutting compared to the HMA in areas where the pavement temperature is expected to be quite high during hot summer days.

Moisture Susceptibility

The moisture susceptibility of foam-stabilised mixes was investigated by submerging specimens in a water bath at 25°C. The average resilient moduli after 24, 48, 72, 96, and 120 hours of water immersion were determined, and subsequently divided by the average resilient modulus values of dry mixes at 25°C, to obtain the Index of Retained Strength (IRS).

The effect of bitumen source and grade on moisture susceptibility was inspected. The foam-stabilised mixes provided excellent moisture resistance as the IRS exceeded 80 to 90% after 5 days soaking. The index values of all mixes were high and varied between sources and grades.

Indirect Tensile Strength

The indirect tensile strength test (ITS) was performed on specimens with different aggregate gradations and mineral fillers. Foam-stabilised mixes using pond ash as a mineral filler showed the lowest ITS value, while those containing fly ash type C, and fly ash type C with 1% cement, showed significant increases in the ITS value. The ITS value for the AC10 HMA is about 3 times the highest ITS value for foam-stabilised mixes. This indicates that fatigue performance of the HMA will be much better than that expected from the foam-stabilised mixes. This can be attributed to the higher binder content in the hot mix asphalt compared to that in the foam-stabilised mixes.

Fracture Energy

The fracture energy of foam-stabilised mixes and AC10 HMA was investigated. This parameter is highly correlated to the fatigue life of the mix. The fracture energy of the HMA is much higher than that of the foam-stabilised mix, and in addition, the AC10 HMA shows much more flexibility than the foam-stabilised mixes, as the ability of the HMA to deform before reaching failure is much higher than that for the foam-stabilised mixes.

Fatigue Life of Foam-stabilised Mixes

The fatigue behaviour of the foam-stabilised mixes was studied using the indirect tensile fatigue test. The fatigue behaviour of both open graded porous asphalt and dense graded HMA was also studied to provide comparison between the behaviour of these different mixes. The dense graded HMA and the open graded porous asphalt provide longer fatigue life than foam-stabilised mixes. However, if in addition to the resilient modulus, some other parameters such as indirect tensile strength or fracture energy are included in the mix design procedure of the foam-stabilised mixes, the fatigue life could be increased by controlling the foam, water content, and the ratio between foam and mineral fillers content that optimise the value of ITS or fracture energy.

California Bearing Ratio (CBR)

California Bearing Ratio was measured for different foam-stabilised mixes using different types of mineral fillers and aggregate gradations. Foamed bitumen stabilisation significantly enhanced the CBR values as the soaked CBR of foam-treated specimens provided higher CBR values than the conventional untreated aggregates. This finding is also evident of the high moisture resistance of the foam-stabilised mixes.

Summary

The foam-stabilised mixes had reasonably good behavioural characteristics in the laboratory and they are expected to perform reasonably well in the field. A more extensive testing programme is required to further investigate the fatigue behaviour of the different categories of the foam-stabilised mixes, and to carry out field calibration of the laboratory-developed models.

Abstract

As the demand for a cost-effective and environmentally friendly pavement stabilisation method increases, so has foamed bitumen stabilisation for unbound granular pavement layers started to gain broad acceptance worldwide.

The second phase of a study on foamed bitumen stabilisation is presented. It is a comprehensive experimental programme, carried out in 2003-2004, to investigate the properties and the expected performance of the foamed bitumen-stabilised mixes.

The experimental work presented compares the foaming characteristics of nine bitumen types from seven different sources. Physical and foamability tests were conducted on all bitumen types to provide a base for comparison between New Zealand sources and overseas sources. A new methodology to characterise the quality of foam is proposed.

Temperature and moisture susceptibilities were studied and compared for different types and grades of bitumen. Volumetric properties, resilient modulus, indirect tensile strength, fracture energy, fatigue life and CBR values were investigated.

1. Introduction to Foamed Bitumen

As the demand for a cost-effective and environmentally friendly pavement stabilisation method increases, so has foamed bitumen stabilisation for unbound granular pavement layers started to gain broad acceptance worldwide.

This report presents the second phase of the foamed bitumen stabilisation study which is to investigate the properties and the expected performance of the foamed bitumen-stabilised mixes, also called foam-stabilised mixes.

In the first phase (Saleh & Herrington 2003), the research team investigated the feasibility of using foamed bitumen as a potential stabilising technique. Preliminary tests were carried out to evaluate the properties of these mixes.

For this second phase of the research, carried out in 2003-2004, a comprehensive testing programme has been conducted to inspect and characterise the behaviour of the foam-stabilised mixes.

Nine bitumen types from seven different sources were examined for their rheological properties. The susceptibility to changes in temperature (i.e. their temperature susceptibility) of the nine bitumen types was evaluated using three different approaches (explained in Section 1.1).

1.1 Rheology of Bitumen

Rheology involves the study and evaluation of the time-temperature dependent response of materials, such as bitumen, that are stressed or subjected to an applied force. As discussed by Roberts et al. (1991), rheological properties of bitumen consist of age hardening, temperature susceptibility, shear susceptibility, stiffness, penetration, ductility, and viscosity. This present study places the emphasis only on temperature susceptibility, penetration, viscosity and softening point as they are closely related.

Temperature susceptibility is defined as the rate at which the consistency[2] of bitumen changes with a change in temperature. Three approaches to characterise this property are Penetration Index (PI), Penetration-Viscosity Number (PVN), and Viscosity-Temperature Susceptibility (VTS) (Roberts et al. 1991). Low PI, low PVN, and high VTS values are indicators of a binder that is highly susceptible to temperature changes (i.e. high temperature-susceptibility) and vice versa (i.e. indicating the bitumen has lower temperature susceptibility). This study included bitumen consistency tests such as penetration, softening point, and viscosity in accordance with ASTM D5, ASTM D36, and ASTM D4402 respectively.

[2] Consistency describes the degree of fluidity of bitumen at any particular temperature.

1.2 Rheological Properties of the Bitumen Samples

Consistency of bitumen is a major physical criterion in explaining bitumen rheological properties. Consistency tests involved in this investigation were penetration, viscosity and softening point. Both penetration and viscosity were carried out at different temperatures to investigate the temperature susceptibility of the bitumens from different sources in order to explain the effects of bitumen rheological properties on the bitumen foaming characteristics and the properties of the resulting mixtures. The study examined the relationship between the physical properties of the bitumen and the foamability characteristics of the resulting foam.

The results of bitumen consistency and bitumen foaming tests of the collected samples are presented in the following paragraphs. The results obtained from these tests were correlated to investigate the significance of rheological properties of bitumen on foaming characteristics and the behaviour of the foam-stabilised mixes, as will be discussed later in this report.

The ability of the system currently used to characterise the quality of the foam was examined by comparing the different sources of foam, their properties, and their ability to effectively mix with aggregate particles.

1.3 Consistency Test Results

Table 1.1 summarises the physical properties of the bitumen samples. Bitumens from seven different bitumen sources were collected and examined in this study. Five bitumens were obtained from three sources (SHL, VEN, and DLT, with different penetration grades) that are currently used in New Zealand, three were from three sources in California in the United States (AR2000, AR4000-1, and AR4000-2), and one (C170) from Australia.

The sources of the New Zealand samples are denoted by letters, and the grades are indicated by numbers (80, 180) using the penetration grade system. Thus the five samples are SHL80, SHL180, VEN80, VEN180, and DLT80.

Samples from the US are graded with the "Aged Residue" (AR) method. The numerical values of this grading system describe the viscosity (in poises) of these samples at 60°C after being aged in the Rolling Thin Film Oven (RTFO) test. Thus the three US samples are AR2000, AR4000-1, and AR4000-2.

For the Australian bitumen, the numerical value of C170 is the viscosity of the original bitumen (in Pa.s) measured at 60°C.

Table 1.1 lists the penetration and viscosity values measured at different temperatures, and the softening points of all the samples.

Table 1.1 Results of consistency tests of the 9 bitumen types from 7 different sources.

Bitumen Type	Penetration		Viscosity		Softening Point (°C)
	Temperature (°C)	Reading (dmm)	Temperature (°C)	Reading (mPa.s)	
SHL80	20	60	80	17500	47
	25	86	95	4810	
	30	142	110	1671	
			135	435	
			150	218.8	
SHL180	15	52	80	7125	39
	20	97	95	2285	
	25	169	110	864.3	
			135	250	
			150	138.8	
VEN80	20	53	80	27500	47.5
	25	78	95	7150	
	30	123	110	2290	
			135	550	
			150	268.8	
VEN180	18	92	80	8100	38
	21.5	129	95	2425	
	25	187	110	925	
			135	261.2	
			150	150	
DLT80	20	45	95	5700	45
	25	76	110	1925	
	30	135	120	1001	
			135	427.5	
AR2000	20	39	80	9550	38
	25	74	95	2470	
	30	141	110	780	
			135	190	
			150	100	
AR4000-1	20	26	80	19800	49
	25	43	95	4385	
	30	80	110	1360	
			135	276	
			150	136	
AR4000-2	20	29	80	17650	48
	25	55	95	4430	
	30	102	110	1450	
			135	310	
			150	155	
C170			60	121162	42.5
	20	36	70	55500	
	25	61	80	18300	
	30	119	90	7162	
			100	3190	
			110	1563	

1.4 Temperature Susceptibility of the Bitumen Samples

Three approaches were used to characterise the temperature susceptibility of the bitumen from the different sources: Penetration Index (PI), Penetration-Viscosity Number (PVN), and the Viscosity-Temperature Susceptibility (VTS). Later in this report, the temperature susceptibilities of the foam-stabilised mixes were measured and compared with the temperature susceptibilities of the bitumens to investigate the sensitivity of these mixes to the bitumen properties. Table 1.2 shows the fitted penetration and viscosity with temperature. Both the standard error (S) and correlation coefficient (r) values confirm that the fitted lines are valid as the correlation coefficients are quite close to 1 (one).

Table 1.2 Fitted lines for penetration and viscosity for bitumens from different sources.

Bitumen Type	Penetration Fitted Lines (Log Pen =)	S	r	Viscosity Fitted Lines (Log Vis =)	S	r
SHL80	1.02988 + 0.0370*T	0.02530	0.995	6.3387 – 0.02731*T	0.10650	0.993
SHL180	0.9271 + 0.05235*T	0.01571	0.999	5.7515 – 0.02468*T	0.09513	0.993
VEN80	0.993 + 0.03636*T	0.01230	0.999	6.6605 – 0.02891*T	0.11240	0.993
VEN180	1.1717 + 0.0439*T	0.00590	1	5.8225 – 0.0250*T	0.10701	0.991
DLT80	0.6990 + 0.04757*T	0.00900	1	6.4265 – 0.02834*T	0.03639	0.998
AR2000	0.4748 + 0.05580*T	0.00070	1	6.1726 – 0.02863*T	0.12393	0.991
AR4000-1	0.4387 + 0.04847*T	0.02100	0.998	6.68406 – 0.0312*T	0.12850	0.992
AR4000-2	0.370 + 0.05469*T	0.00399	1	6.5306 – 0.02968*T	0.11080	0.993
C170	0.51781 + 0.05151*T	0.02510	1	7.42629 – 0.03905*T	0.06000	0.996

1.4.1 Penetration Index (PI)

The Penetration Index (PI), one of the three methods for characterising temperature susceptibility, can be determined by drawing the relationship between penetration values on a log scale and the corresponding temperatures on an arithmetic scale. Based on the slope (gradient) of the penetration–temperature fitted line, the Penetration Index (PI) of each sample was calculated using Equation 1. The results are shown in Table 1.3 and depicted in Figure 1.1.

$$PI = \frac{20 - (500 \times slope)}{1 + (50 \times slope)} \qquad \text{Equation 1}$$

Table 1.3 Penetration indices (PI) of the bitumens from different sources, arranged in order of decreasing PI (increasing temperature susceptibility).

Bitumen Type	Slope	PI
VEN80	0.03636	0.65
SHL80	0.03700	0.53
VEN180	0.04390	–0.61
DLT80	0.04757	–1.12
AR-4000-1	0.04847	–1.24
C170	0.05151	–1.61
SHL180	0.05235	–1.71
AR-4000-2	0.05469	–1.97
AR-2000	0.05580	–2.08

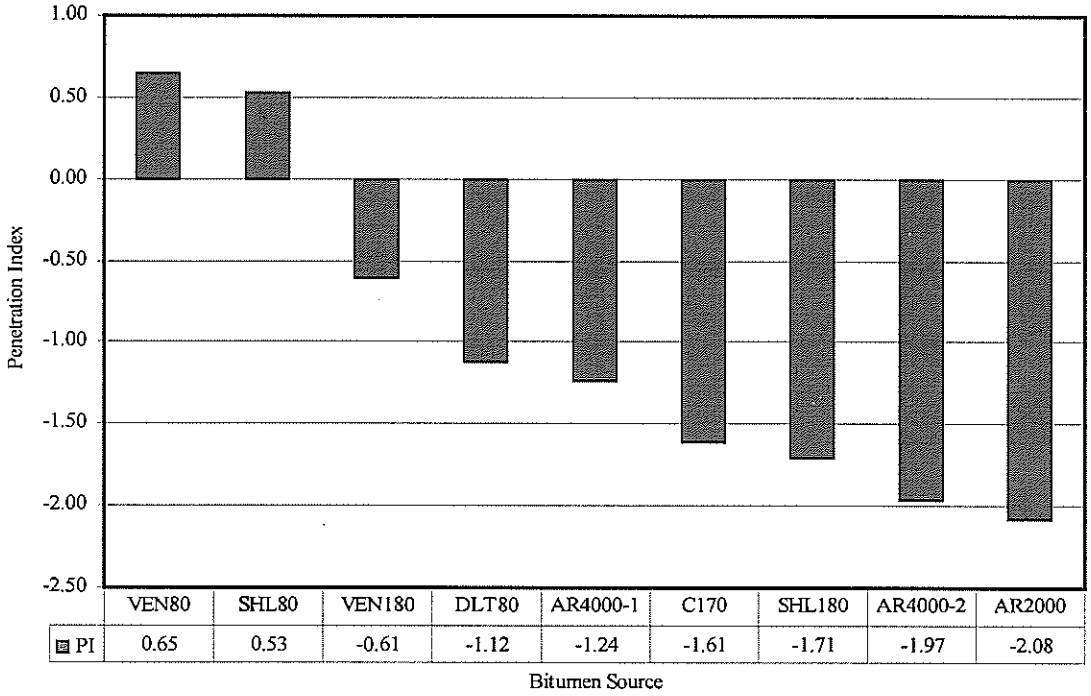

Figure 1.1 Penetration indices of the bitumens from different sources, shown graphically.

Figure 1.1 shows that the PI values are between –2.08 and +0.65. According to Roberts et al. (1991), PI values for most good paving binders are between +1 and –1. High temperature susceptibility occurs when the binder has PI below –2. AR2000 shows the lowest PI value while VEN80 exhibits the highest PI. Therefore, AR2000 is the most temperature-susceptible binder. Such a binder is vulnerable to brittleness, leading to cracks in cold climate areas and prone to rutting at high temperatures. In addition, those binders also have low viscosity at 135°C leading to tender mix problems (such as instability leading to distortion and rutting) during compaction under traffic loads (Roberts et al. 1991). Table 1.3 also shows that all New Zealand bitumens, except SHL180, have reasonably low temperature susceptibilities.

1.4.2 Penetration-Viscosity Number (PVN)

This second method is based on penetration at 25°C and viscosity at either 135°C or 60°C, which are standard specifications for paving bitumen. Equation 2 was used to calculate PVN of each bitumen sample (Roberts et al. 1991):

$$PVN = \frac{L - X}{L - M}(-1.5) \qquad \text{Equation 2}$$

where:

X = the logarithm of viscosity in centistokes measured at 135°C
L = the logarithm of viscosity at 135°C for a PVN of 0.0
M = the logarithm of viscosity at 135°C for a PVN of –1.5

The values of L and M can be determined using the equations below (based on the least square fits).

The equation for the line representing a PVN of 0.0 is:

L = log (Vis @ 135°C) = 4.258 – 0.7967 * log (Pen at 25°C) Equation 2a

The equation for the line representing a PVN of –1.5 is:

M = log (Vis @ 135°C) = 3.46289 – 0.61094 * log (Pen at 25°C) Equation 2b

Note that this study assumed a specific gravity of all bitumen samples equal to 1 (one). The relationship between viscosity units is therefore:

1 centipoise = 1 mPa.s = centistokes * bitumen specific gravity.

Table 1.4 shows the values of X, L, and M, and Figure 1.2 shows PVN values of all nine different bitumen types.

Table 1.4 Penetration-viscosity numbers (PVN) of the nine bitumen types, arranged in order of decreasing PVN (lowest temperature susceptibility to highest).

Bitumen Type	X	L	M	PVN
VEN80	2.75765	2.742674	2.300880	0.050846
VEN180	2.44750	2.450121	2.076539	–0.01052
SHL80	2.65185	2.701055	2.268965	–0.17082
SHL180	2.41970	2.476954	2.097116	–0.22610
DLT80	2.60060	2.753643	2.309291	–0.51663
AR4000-2	2.52380	2.873915	2.401521	–1.11173
AR4000-1	2.47206	2.943123	2.454592	–1.44637
AR2000	2.30755	2.768316	2.320543	–1.54353
C170	2.15454	2.819368	2.359692	–2.16944

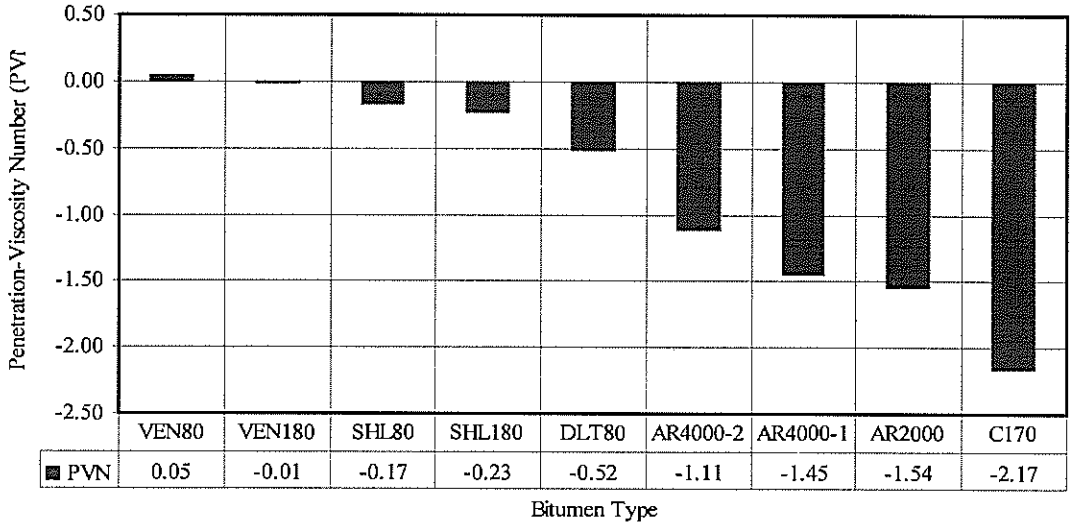

Figure 1.2 Penetration-viscosity numbers (PVN) of the nine bitumen types, shown graphically.

Figure 1.2 shows that all PVN values were between +0.05 and –2.17. According to Roberts et al. (1991), most paving binders have a PVN between +0.5 to –2.0. Bitumen class C170 showed the lowest PVN value, while VEN80 exhibited the highest. Thus, C170 is the most temperature-susceptible binder and VEN80 is the least temperature-susceptible bitumen. It is also clear that these bitumens used in New Zealand have lower temperature susceptibility compared to US bitumens, as all the three US types lie within the high temperature-susceptibility range.

1.4.3 Viscosity-Temperature Susceptibility (VTS)

The Viscosity-Temperature Susceptibility (VTS) value for measuring temperature susceptibility for any particular bitumen sample was determined using the following equation:

$$VTS = \frac{\log(\log \text{Vis at } T_2) - \log(\log \text{Vis at } T_1)}{\log T_1 - \log T_2} \qquad \text{Equation 3}$$

where:

T = the bitumen temperature in degrees Kelvin (°K = 273 + °C).

Table 1.5 was then constructed and portrayed in Figure 1.3.

Figure 1.3 shows that all VTS values are between 4.60 and 8.80. C170 bitumen shows the highest value, while SHL180 exhibits the lowest. Thus, C170 is the most temperature-susceptible bitumen. Also, Figure 1.3 shows that all New Zealand bitumens have reasonably low temperature susceptibilities according to their VTS values. Once again US bitumens show high temperature susceptibility, with AR4000-1 being the worst according to its VTS value.

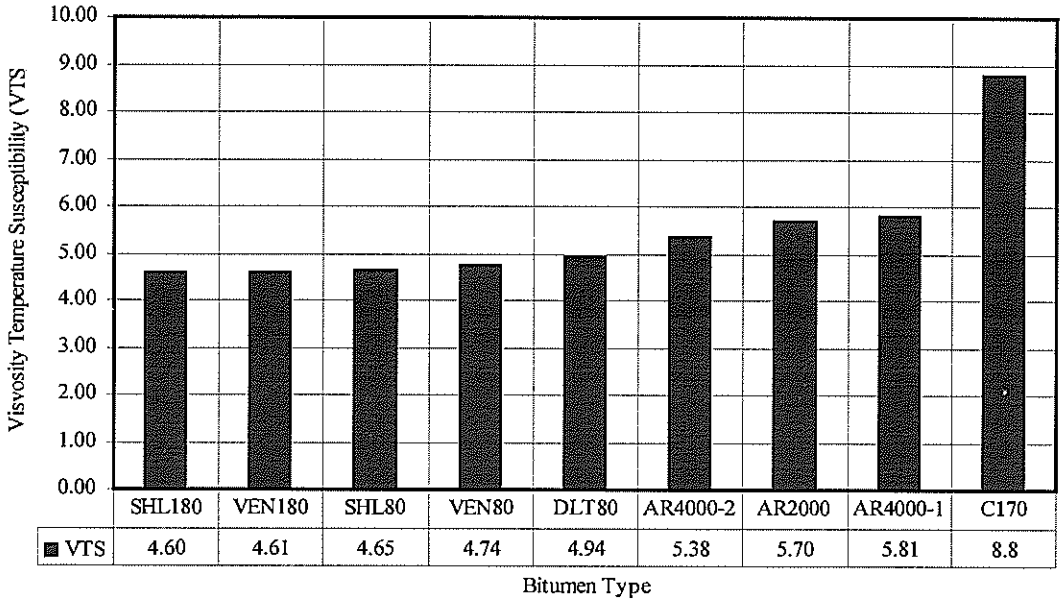

Figure 1.3 Viscosity-temperature susceptibility (VTS) of the nine bitumen types, shown graphically.

Table 1.5 Viscosity-temperature susceptibility (VTS) of the uine bitumen types, arranged in order of increasing VTS (lowest temperature susceptibility to highest).

Bitumen Type	VTS
SHL180	4.60
VEN180	4.61
SHL80	4.65
VEN80	4.74
DLT80	4.94
AR4000-2	5.38
AR2000	5.70
AR4000-1	5.81
C170	8.80

1.4.4 Summary of Methods

Each of the three approaches used to determine the temperature susceptibility resulted in a different order of the least and the most temperature-susceptible bitumens.

Nonetheless, results from all the three methods show that the C170 and US bitumens have higher temperature susceptibilities compared to the New Zealand bitumens. The differences between the results of the three approaches may be attributed to the empirical nature of the penetration test. Since viscosity is a fundamental property of bitumen, it provides more reliable results than penetration.

Also, it is noticeable that DLT80 is the most temperature-susceptible bitumen type compared to the other New Zealand types used in this study.

Later in this report, the temperature susceptibility of the different binders was compared with the characteristics of the resulting foamed bitumens and was examined against the temperature susceptibility of the resulting foam-stabilised mix.

2. Properties of Bitumen Foams

2.1 Preparing the Foamed Bitumen

The Wirtgen WLB10 unit, a laboratory-scale foamed-bitumen plant, was used to determine the foaming properties of the different types of bitumens, and to produce foamed bitumen required to treat the aggregate (AP-20 and AP-40) samples. The foamed bitumen was used for the classification tests that measure the quality of the foam, and determine its suitability for mixing with aggregates. The details of the foamability parameters are described in detail in Saleh & Herrington (2003). A brief summary of the foamability test parameters and the use of the WLB10 portable foaming laboratory unit follows.

In preparing the unit to produce the bitumen foam, the water tank is filled with water, and the air and power supply is turned on. A sufficient amount of liquid bitumen (±10 kg) is poured into the pre-heated tank. The bitumen is then circulated. Whenever a different bitumen source or grade is used the bitumen discharge flow rate has to be calibrated. The calibration is done by discharging the bitumen for a certain period of time, and subsequently measuring the weight of the discharged bitumen. Table 2.1 gives an example of measuring the flow rate of bitumen in the foaming machine.

Table 2.1 Calculation of bitumen flow rate in the Wirtgen WLB10 foaming unit.

Discharge Time (sec)	Bitumen weight (g)	Flow rate (Q_b) (g/sec)
5	463.0	92.60
4	361.0	90.25
3	258.5	86.17
2	194.1	97.05
1	92.0	92.00
	Average flow rate	**91.61**

Table 2.1 shows that the average flow rate of that particular bitumen is 91.61 g/sec. As exactly 500 grams of foamed bitumen are needed for the foaming test, the automatic timer is set to 500/91.61, i.e. 5.46 seconds.

Based on the bitumen flow rate, the foamant-water flow rate for each percentage of water content is calculated with the following equation:

$$Q_w = \frac{Q_b * W_c * 3.6}{\gamma_b * 100} \qquad \text{Equation 4}$$

where:

Q_w = water flow rate (litre/hour)
Q_b = bitumen flow rate (gram/second)
W_c = percentage of foamant water
γ_b = bitumen density (assumed to be 1 g/cm^3)

Table 2.2 gives the foamant water flow rates corresponding to particular percentages of the foamant water content.

Table 2.2 Calculation of foamant water flow rate according to % foamant water content (W_c).

Percent water content (% W_c)	2	2.5	3	3.5	4
Q_w (litres/hour)	6.6	8.25	9.89	11.54	13.19

After setting the foamant water flow rate, the air and water pressure are adjusted. A standard metal bucket is then placed under the nozzle. A standard dipstick is held vertically and placed inside the bucket. With visual inspection of the height of the foamed bitumen on the dipstick, the expansion ratio (ER) is determined. Normally the foam surface profile is irregular and, therefore, the average level of the surface is considered as the ER. The half-life time (HLT) is measured using a stopwatch from the moment that maximum expansion is reached until the bitumen collapses to half of the maximum volume, as measured on the dipstick. This allows the half-life time to be calculated.

2.2 Tests to Characterise Bitumen Foams

In evaluating the foam characteristics, the ER and HLT values were used. Table 2.3 contains the foaming parameters and the results of all bitumen types used in this study. The foam index (FI) was calculated from the following equation (Jenkins et al. 2000):

$$FI = \frac{-\tau_{1/2}}{\ln 2} * \left(4 - ER - 4 * \ln\left(\frac{4}{ER}\right)\right) + \left(\frac{1+c}{2c}\right) * ER * t_s$$

where:

t_s = discharge time (in seconds): in this research, t_s value is 5 seconds.
c = ratio of measured and actual ER; this can be determined from the relevant chart in the South African (SA) Interim Technical Guidelines (SA Transportek 2002).

Figure 2.1 shows the relationship between the percentages of foamant water and the corresponding FI values for different bitumen sources. The water content that maximises the FI is the optimum foamant water content. As it appears from Figure 2.1, most of the bitumen sources do not show any peak. In this case, the percentage of water that generated a half-life equal to or greater than 7 seconds was considered the optimum. Table 2.4 gives the optimum percentage of foamant water of each sample that was used later in the preparation of foam-stabilised specimens. In addition, the FI values for the corresponding optimum foamant water are presented and subsequently assessed for cold mix use (based on SA Transportek 2002).

Figure 2.1 shows that the use of the FI to optimise the percentage of foamant water is not achievable in most tests because very few bitumen types show a peak. This may be attributed to the fact that the FI was developed assuming that the rate of decay of the foam follows a certain exponential decay curve (Equation 5), which may not be valid for all bitumen types. In addition, the FI value relies on the expansion ratio and the half-life, which are both empirical parameters. Therefore, FI is also an empirical

parameter. Because of the empirical nature of the current parameters that are in use to characterise the foam quality, several discrepancies in classification of the different sources of foam bitumen can be detected. For example, although DLT80, SHL80 and AR4000-2 were classified as poor or unsuitable for foam stabilisation (Table 2.4), they both mixed and dispersed effectively with the aggregate matrix in the laboratory without any problems. However C170 did not mix.

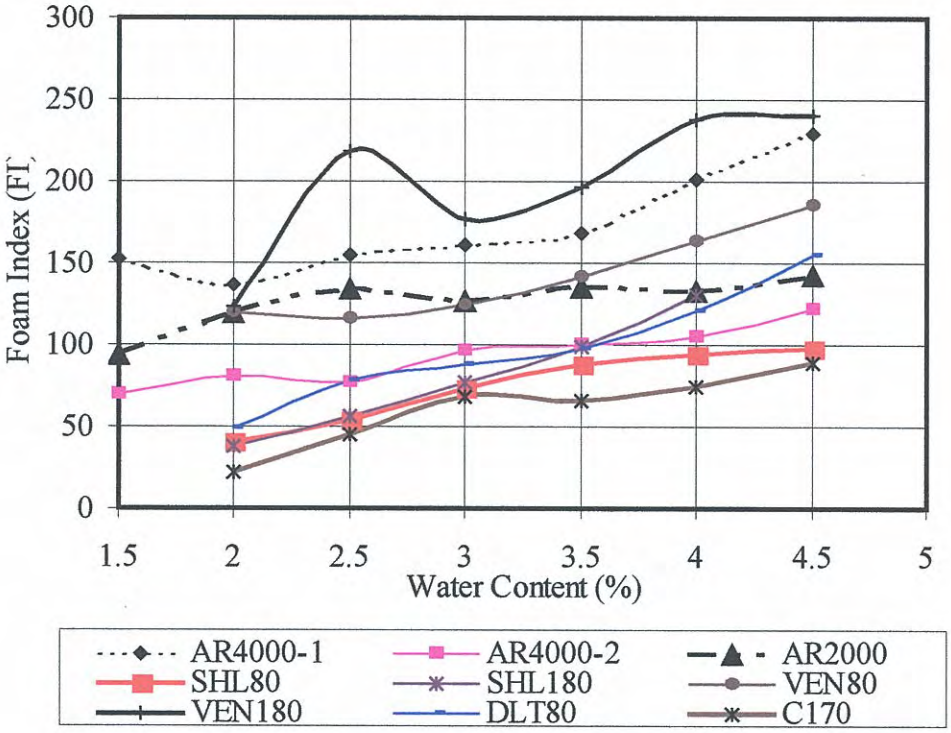

Figure 2.1 Relationship between Foam Index (FI) and water content (Wc) of the bitumen samples.

According to Figure 2.1, VEN180 provides the best quality foam and C170 gives the lowest quality foam. It was not possible to mix the foam created from C170 since the foam formed clots and strings and, therefore, no specimens could be prepared for it.

Despite the disadvantages of the foam classification system currently used, it has several advantages such as:

1. Simplicity of measurements;
2. Inexpensive equipment to measure the expansion ratio and half-life;
3. Reasonable classifications (but care should be taken in specifying limits for expansion ratio, half-life, and foam index as they will differ from one bitumen source to the other); and
4. Measurements can take place on site.

Table 2.3 Foaming properties of the nine different bitumen types.

%W_c	ER	HLT	FI	%W_c	ER	HLT	FI
	SHL80				SHL180		
2.0	6	12.7	40.0	2.0	5.8	10.4	37.4
2.5	7.7	6.2	53.4	2.5	7.6	9.5	56.4
3.0	9.7	4.7	72.8	3.0	9.3	8.8	77.3
3.5	11	3.5	88.4	3.5	11.3	7.6	99.1
4.0	12	4.0	93.4	4.0	13.9	7.2	130.7
4.5	12	3.2	97.5	4.5			
%W_c	VEN80			%W_c	VEN180		
2.0	12.0	10.3	119.7	2.0	9.7	23.7	123.5
2.5	12.5	8.0	115.6	2.5	15.3	16.0	218.4
3.0	13.3	7.5	124.6	3.0	18.0	6.3	176.6
3.5	15.3	5.7	141.9	3.5	20.0	5.7	196.7
4.0	17.7	4.9	163.5	4.0	24.0	5.0	237.9
4.5	20.0	4.3	185.1	4.5	24.0	5.2	240.2
%W_c	DLT80			%W_c	AR2000		
2.0	7	8	48.4	1.5	11	8.9	94.4
2.5	10	3	78.2	2.0	12	10.3	119.9
3.0	11	3	87.7	2.5	16	5.5	134.4
3.5	12	4	97.0	3.0	17	3.6	127.1
4.0	14	5	121.0	3.5	18	3.6	135.9
4.5	17	5	155.2	4.0	18	3.2	132.4
				4.5	19	3.1	142.2
%W_c	AR4000-1			%W_c	AR4000-2		
1.5	11	23.8	152.2	1.5	10	7.3	69.63
2.0	14	8.8	137.0	2.0	11	6	80.06
2.5	17	5.7	155.3	2.5	11	4.7	77.35
3.0	18	4.6	160.5	3.0	12	6.7	96.38
3.5	18	5.2	168.6	3.5	13	6.4	100.32
4.0	21	5.5	201.2	4.0	14	5.2	104.87
4.5	23	5.1	229.4	4.5	16	4.6	121.36
%W_c	C170						
2.0	3	32	22.1				
2.5	6	27.3	45.5				
3.0	7	30.4	68.8				
3.5	8	12.8	66.2				
4.0	9	9.7	74.5				
4.5	11	3.0	89.4				

Note:
ER Expansion Ratio HLT Half-life in seconds
FI Foam Index

Table 2.4 Optimum foamant water content, FI, and Foam Classification* of the nine bitumen types (in order of decreasing FI, or decreasing suitability for foaming).

Bitumen Type	% Optimum Foamant Water	Foam Index	Foam Classification
VEN180	2.6	224	Very Good
AR4000-1	2	143.5	Good
AR2000	2	118.6	Moderate
VEN80	3	114.9	Moderate
SHL180	3.5	109	Moderate
AR4000-2	2	89.7	Poor
C170	3.5	66	Unsuitable
SHL80	2.5	55.7	Unsuitable
DLT80	2	48.4	Unsuitable

* The quality of foam and its suitability to be used and mixed with aggregates.

Examining Table 2.4, the optimum percentage of foamant water for each sample is within the range of 1 to 3.5 that was recorded in the literature (Maccarrone et al. 1994, Mohammad et al. 2003, Ramanujam & Jones 2000). Under the same testing conditions, the effect of bitumen source is also obvious. For instance, AR4000-1 and AR4000-2 are supposed to have similar physical properties and yet they have different foamability parameters.

2.3 Relationship between Physical Properties of Bitumen and its Foamability

All nine bitumen types were sorted in ascending order based on viscosity at 135°C, and are shown in Table 2.5. Although there are inconsistencies, generally soft binders, except C170, produced reasonable foam, and harder binders such as AR4000-2, SHL80 and DLT80 produced low quality or unsuitable foams, according to the current CSIR classification system.

Table 2.5 Relationship between bitumen viscosity at 135°C of the bitumen samples, and their foam quality (in order of increasing viscosity).

Bitumen Type	Viscosity at 135°C (mPa.s)	Foam Classification
C170	143	Unsuitable
AR-2000	203	Moderate
SHL180	263	Good
VEN180	280	Very Good
AR-4000-1	297	Good
AR-4000-2	334	Poor
DLT80	399	Unsuitable
SHL80	449	Unsuitable
VEN80	572	Moderate

Based on Tables 1.4 and 2.4, Table 2.6 was constructed. The table lists each sample from the least to the most temperature susceptible, based on the PVN approach, and the corresponding foam classification.

Table 2.6 Relationship between temperature susceptibility and foaming quality (in order of decreasing PVN).

Bitumen Type	PVN	Foam Classification
VEN80	0.05	Moderate
VEN180	–0.01	Very Good
SHL80	–0.17	Unsuitable
SHL180	–0.23	Good
DLT80	–0.52	Unsuitable
AR4000-2	–1.11	Poor
AR4000-1	–1.45	Good
AR2000	–1.54	Moderate
C170	–2.17	Unsuitable

It is obvious that C170 is the most temperature-susceptible binder and produces unacceptable foam, while AR2000, which is also highly temperature-susceptible, shows reasonable foaming characteristics that were similar to those produced by VEN80 (which is the least temperature-susceptible binder). The conclusion is that the use of temperature-susceptible binders does not have a direct effect on the foaming properties. However, detrimental effects may be derived from the resulting mixtures of foamed bitumen and aggregates, which were assessed later in this research.

2.4 New Approach to Characterising Foam Bitumen Quality

The lack of a consistent methodology that employs fundamental parameters to classify the quality of the foam, prompted the researcher of this project to suggest another procedure to quantify the foam quality. In this new approach, the Brookfield rotational viscometer (Figure 2.2) was connected to a computer, and the foam viscosity was measured every half second interval, for about three to four minutes. Figure 2.3 shows the relationship between the rotational viscosity of the foam, which was created by the addition of 2.5% water to SHL80 bitumen, and the elapsed time in seconds. The average foam viscosity over the first 60 seconds was calculated, and shown in Figure 2.3. This value is considered a relevant parameter to quantify the foam quality. The first 60-second interval represents the mixing time in the laboratory.

Figure 2.2 Brookfield rotational viscometer used for quantifying foam quality.

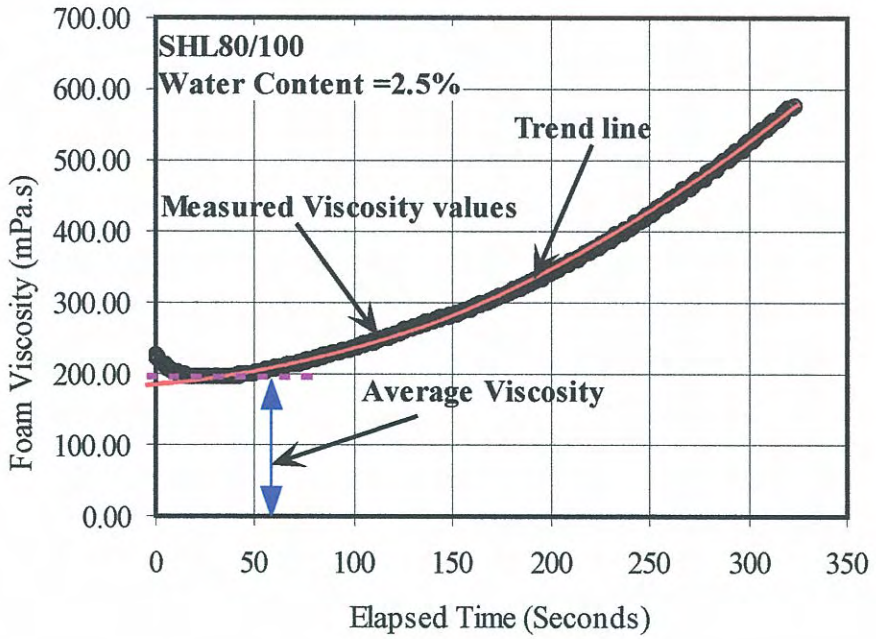

Figure 2.3 Relationship between foam viscosity and elapsed time.

For the purpose of characterising the quality of the foam bitumen, this approach is likely to be more appropriate than the current approach, which relies on empirical parameters such as expansion ratio, half-life and FI. Because viscosity of the foam is a fundamental property, this new approach will provide a direct measurement of the viscosity of the foam and, therefore, will provide a good understanding of the workability and the mix quality. The current empirical parameters only provide an indication about the viscosity of the foam, but do not give an exact figure about its value. In addition, the current empirical parameters may provide inconsistent measures. For example, two different sources of bitumens may have the same expansion ratio and half-life, but might have totally different foam viscosity values, which makes the mixing quality and workability of the two different mixes completely different.

In hot mix asphalt (HMA) design, the ASTM D5581-96 standard requires the viscosity of the bitumen at the mixing time to be around 170 ±20 Centistokes with a range of 150 to 190 mPa.s, assuming the density of bitumen 1 g/cm^3. Note that in HMA mix design, the aggregate is at the same temperature of the bitumen (or even higher to compensate for the temperature loss during mixing) to ensure that mixing occurs when the binder is in the optimal viscosity range. However, this is not the case with foam-stabilised mix design since the hot foam is blended with the moist cold aggregate. Therefore, the temperature of the foam during mixing will change based on the aggregate temperature, and will reach what may be called an "equilibrium temperature". The viscosity of the foam at this equilibrium temperature is significant since it will affect the ability of the foam to mix with the aggregate. In this research project, the concept of measuring the foam viscosity at different time intervals and the determination of the average viscosity over the first minute will be introduced. More research, however, will be required to account for the aggregate temperature in order to set minimum and maximum limits for the viscosity of the foam, and to classify the quality of the foam.

2.5 New Approach to Determining Optimum Foamant Water Content

This new approach assumes that the optimum foamant water is that which produces the lowest rotational viscosity (measured by the Brookfield rotational viscometer) of the foam.

The average viscosity over a period of 60 s was computed for different foamant water contents. The relationship between the percentage of water content and average viscosity was then plotted as shown in Figures 2.4 to 2.10. The water content that produces the minimum viscosity is then considered the optimum foamant water content. As shown in Figures 2.4 to 2.10, for almost all the different sources of bitumen, the relationship between foam viscosity and water content has a minimum value for viscosity. Sometimes two minimums can be detected. In such cases, the absolute minimum should be the one of interest.

Some explanations for the discrepancies in the current empirical systems can now be explained with this new approach. For example, according to the empirical parameters (expansion ratio, half-life, and FI), SHL80 was classified as poor, although it was possible to mix it effectively with the aggregate matrix without any

problems. Examining Figure 2.4, the foam viscosity of the SHL80 is about 190 mPa.s, which is good enough to ensure effective mixing. Also, comparing the foam viscosities of SHL80, SHL180, and VEN180, there is no significant difference between them. However, according to the empirical parameters (expansion ratio and half-life) VEN180 was found to be superior compared to SHL80 and SHL180. The same argument can be made for AR4000-2 which was classified as producing a poor foam according to the FI value, although it was later found to mix nicely with aggregate, which can be explained by its reasonable foam viscosity of 250 mPa.s (i.e. close to 150 to 190 mPa.s).

This new approach appears to be more reliable as it is based on a fundamental parameter such as viscosity.

Table 2.7 shows a comparison between the optimum foamant water contents of the current and new approaches. There are some similarities and differences between the results of the two systems for some bitumens. An extensive testing programme is required to inspect the new approach to check the repeatability of the test and establish its reliability.

Table 2.7 Optimum foamant water contents (%) of the current and new approaches.

Bitumen Type	Current Approach	New Approach
SHL80	2.5	2.6
SHL180	3.5	2.5
VEN80	3.0	2.75
VEN180	2.6	2.1
AR2000	2	4.0
AR4000-1	2	4.0
AR4000-2	2	2.2
C170	3.5	N/A

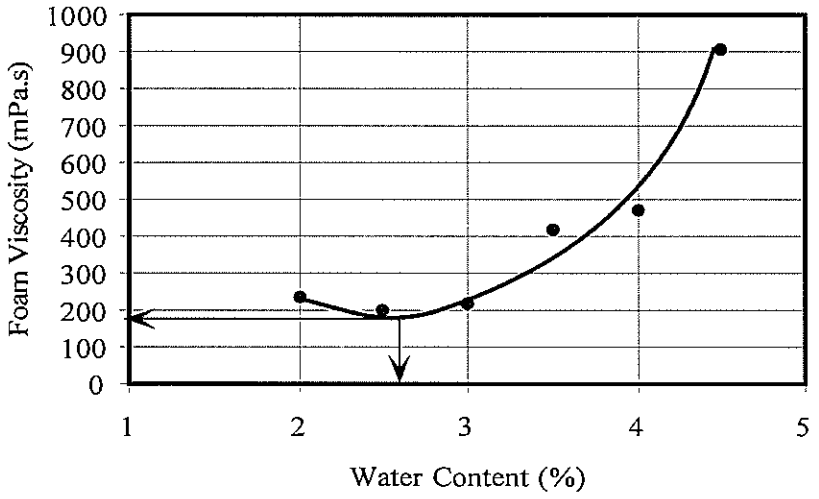

Figure 2.4 Relationship between Foam Viscosity (mPa.s) and % Foamant Water for SHL80 Bitumen.

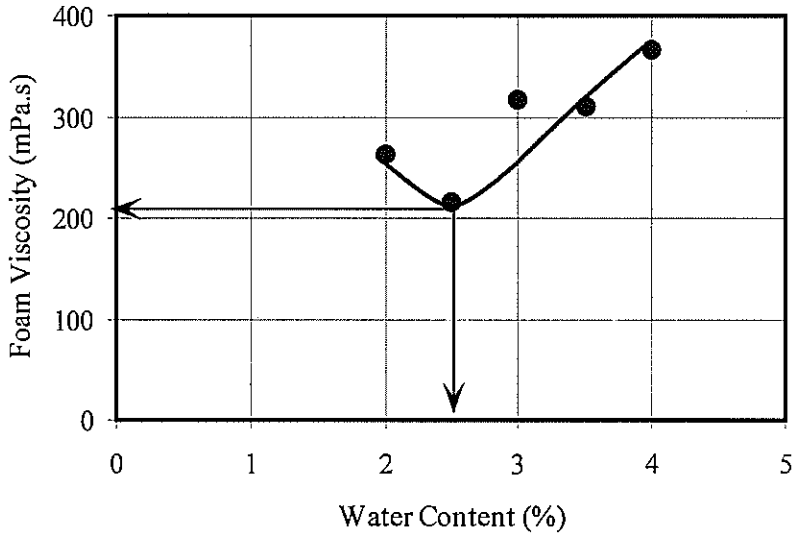

Figure 2.5 Relationship between Foam Viscosity (mPa.s) and % Foamant Water for SHL180 Bitumen.

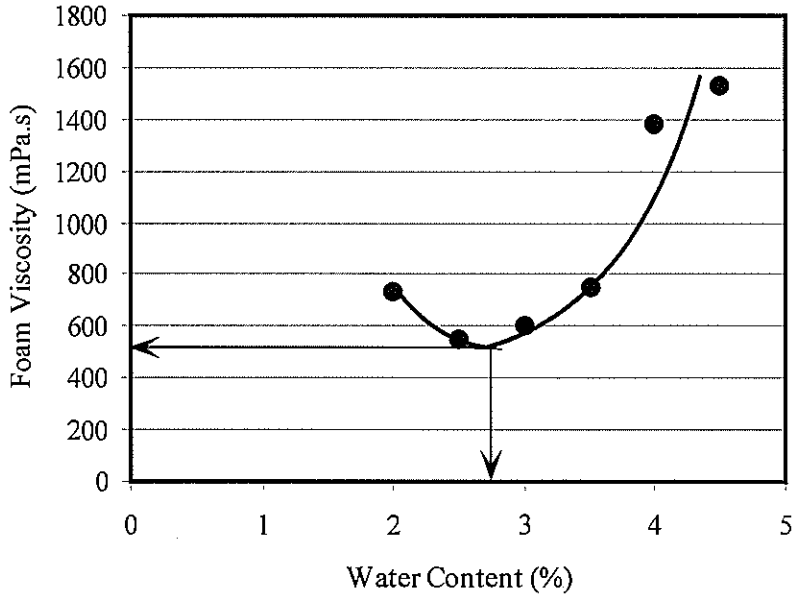

Figure 2.6 Relationship between Foam Viscosity (mPa.s) and % Foamant Water for VEN80 Bitumen.

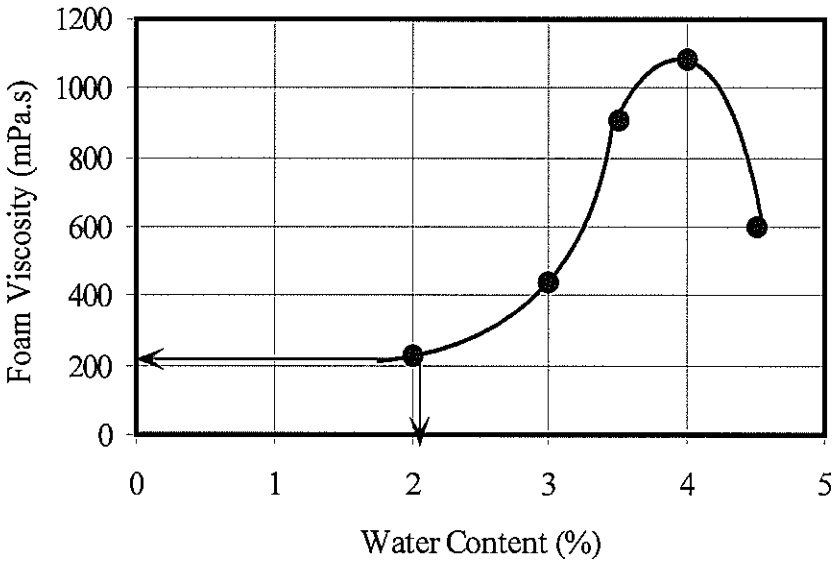

Figure 2.7 Relationship between Foam Viscosity (mPa.s) and % Foamant Water for VEN180 Bitumen.

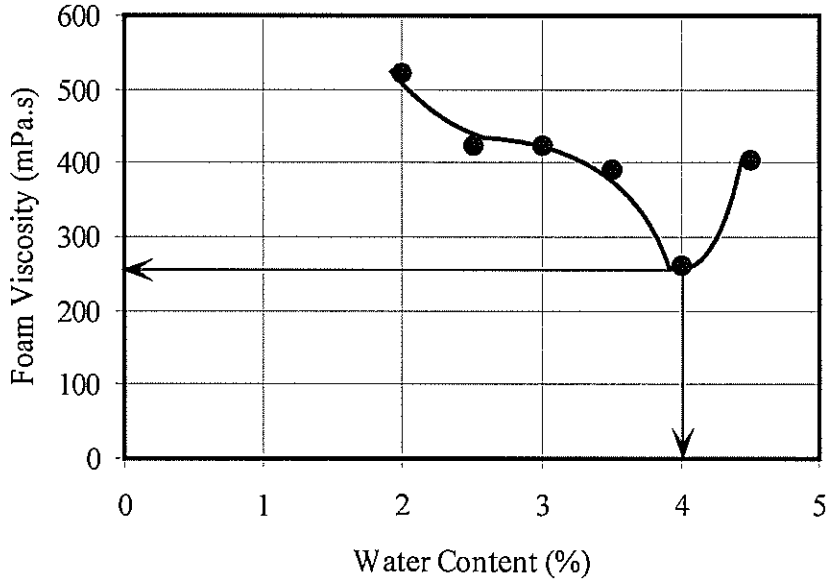

Figure 2.8 Relationship between Foam Viscosity (mPa.s) and % Foamant Water for AR2000 Bitumen.

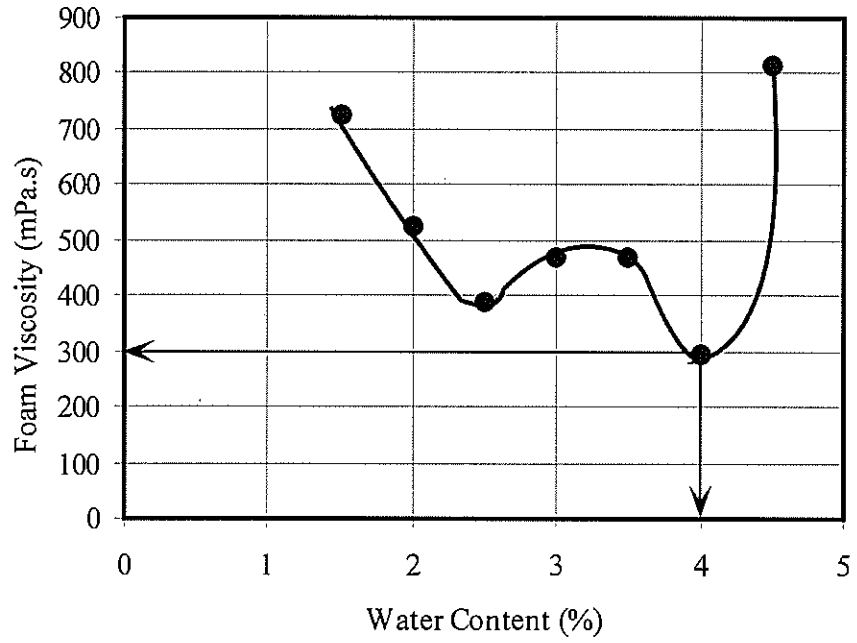

Figure 2.9 Relationship between Foam Viscosity (mPa.s) and % Foamant Water for AR4000-1 Bitumen.

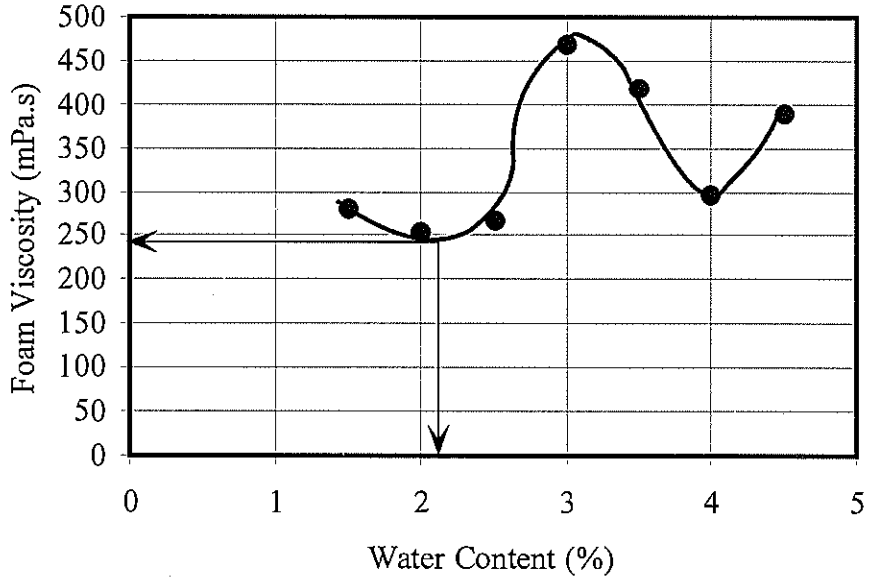

Figure 2.10 Relationship between Foam Viscosity (mPa.s) and % Foamant Water for AR4000-2 Bitumen.

This research indicates that the measurements of average foam viscosity may be a reliable indicator of the quality and suitability of foamed bitumen for mixing. Further research is required to investigate its repeatability and reliability, and the impact of typical field mixing temperatures on bitumen foam viscosity.

3. Foamed Bitumen Mix Design

This chapter presents the determination of aggregate optimum moisture content (OMC) as one of the foamed bitumen mix design parameters. After preparing the mixes at their optimum mixing moisture content (OMMC) and optimum mixing foam content (OMFC), their properties were characterised. The characterisation of the mixes involves resilient modulus measurements, effect of different bitumen sources, effect of aggregate gradation and types of mineral fillers, temperature and moisture susceptibility, indirect tensile strength measurements, California bearing ratio (CBR) test, volumetric properties, and fatigue life.

3.1 Aggregate Optimum Moisture Content (OMC)

The first phase of this research (Saleh & Herrington 2003) investigated three compaction methods that are used to determine the aggregate OMC. They were the Gyratory, Marshall, and Vibratory methods, the laboratory procedures and apparatus for which are described in AS2891.2.2, ASTM D1559, and NZS 4402:1986, respectively. The use of different methods was intended to observe the most suitable method in the preparation of the mixes. The results of these compaction methods are recorded in Saleh & Herrington (2003).

Different amounts of water were added to the oven-dry aggregate to achieve different moisture contents ranging from 4% to 8% with a 1% increment by weight of the dry aggregate. The aggregate OMC is defined as the percentage of moisture content added to the aggregate that yields the maximum dry density. The Gyratory compaction method was utilised to determine the aggregate OMC.

In this second phase study, specimens were compacted using the Gyratory compactor. Two aggregate gradations were used, which are the upper limit of the gradation band of the AP-40 (all passing the 40 mm sieve) and the mid-point of AP-20 gradation curve. These two gradations were selected because they are reasonably close to the mid-point of the ideal zone for foamed bitumen mixes, as shown in Figure 3.1 and discussed in the previous study by Saleh & Herrington (2003). In addition, four types of mineral filler: fly ash type C, Huntly pond ash, hydrated lime, and Portland cement, were used to adjust the amount of fines. The Portland cement was used at 1.0% and 2.0% with fly ash type C.

Huntly pond ash is a by-product of power generation boilers, and can cause an environmental hazard because of its alkalinity, high concentrations of boron, and presence of several heavy metals such as arsenic and cadmium. Using it in foam stabilisation was investigated as a potential safe way of discarding it economically.

Table 3.1 shows the different combinations of AP-40, AP-20, and the mineral fillers that have been investigated. The name of each group has been designated with letters and numbers to indicate the aggregate gradation, the types of filler, and the percentage of Portland cement, if any. For example, M20FA indicates that the mix

contains AP-20 gradation with fly ash as a mineral filler, while M20FA2C is a mix containing AP-20 gradation, fly ash, and 2.0% Portland cement.

The 150-mm diameter specimens were prepared in accordance with AS 2891.2.2 using AP-40 aggregate, 80 gyration cycles, and a 3° gyratory angle. The 100-mm-diameter specimens were prepared using AP-20 aggregate, 80 gyration cycles, 240 kPa air pressure, and 2° gyratory angle. The 150-mm-diameter mould was used for the AP-40 aggregates and the 100-mm-diameter mould was used for the AP-20 aggregates.

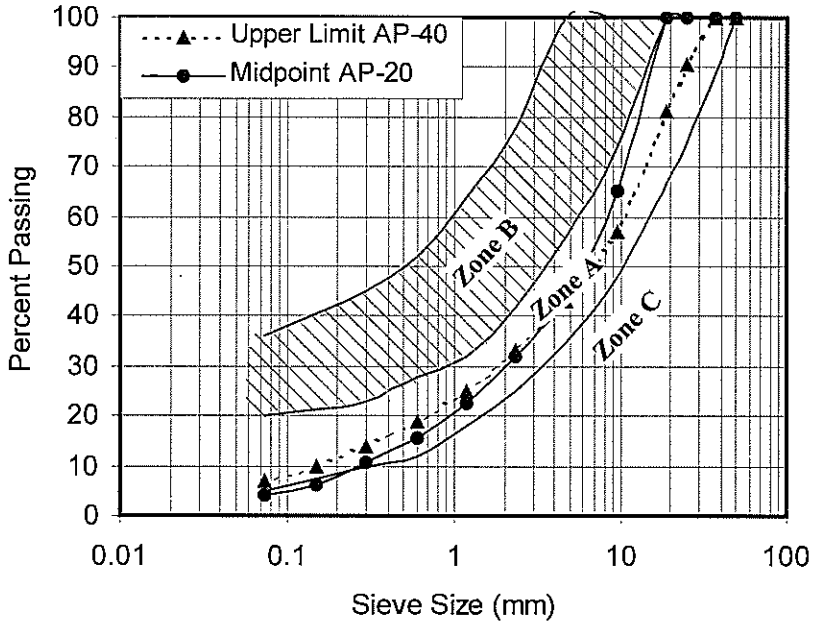

Figure 3.1 Aggregate gradation of mixes and their suitability for use in foamed bitumen mixes.

Figure 3.1 shows three zones A, B, and C. Only gradations comply with zone A are suitable for foam bitumen stabilisation. Gradations close to B or C need to be modified to comply with zone A.

Table 3.1 Names designated to foam-stabilised mixes based on their compositions.

Aggregate Gradation	Type of Mineral Filler				
	Fly Ash Type C (FA)	Fly Ash C + 2.0% Cement (FA2C)	Fly Ash C + 1.0% Cement (FA1C)	Huntly Pond Ash (PA)	Hydrated Lime (LM)
AP-20	M20FA	M20FA2C	M20FA1C	M20PA	M20LM
AP-40	N/A	N/A	N/A	M40PA	M40LM

Table 3.2 shows the aggregate OMC for the different mix types.

Table 3.2 Aggregate Optimum Moisture Content (OMC%) for different foam-stabilised mixes.

Mix	Aggregate OMC (%)
M20 FA	7.20
M20FA2C	6.00
M20PA	6.75
M20LM	6.75
M40PA	6.75
M40LM	6.75

3.2 Mixing Moisture Content (MMC) and Mixing Foam Content (MFC)

3.2.1 Preparation of Samples

The mixing moisture content (MMC) is the amount of water contained in a mix before the addition of the foamed bitumen.

The dry aggregate was mixed with water at a range of different percentages of MMC, then mixed with foam at a range of different percentages of MFC, and subsequently compacted using the Gyropac compactor. Curing took place at room temperature for seven days and the readings of resilient modulus were taken after every 24 hours of the curing period.

The full details of the resilient modulus test are given in AS2891.13.1-1995. A brief description of the resilient modulus test can be found in the report by Saleh & Herrington (2003) for the first phase of this research.

The mixtures were then oven-dried until a constant weight was achieved, at which point the ultimate resilient modulus was determined. The M_r value of the dry specimens was later compared with the resilient modulus obtained on Day 7, to determine the adequacy of curing for seven days at room temperature in achieving the ultimate resilient modulus.

Figure 3.2 Foam-stabilised specimens prepared using the Gyropac compactor.

For the foam-treated AP-40 gradation, specimens were prepared with combinations of four MMC values of 70%, 80%, 100% and 120% of the aggregate OMC, and four MFC values of 2.5%, 3.0%, 3.5% and 4.0% by weight of the dry aggregate. Figure 3.2 shows the specimens made for the two series, one with lime and one with Huntly pond ash as the mineral fillers, for these combinations.

3.2.2 Optimum Mixing Moisture and Mixing Foam Contents

The approach using simultaneous determination of OMMC and OMFC, which was discussed in the first report of this study (Saleh & Herrington 2003), was used. In the previous report, the contour lines of the resilient moduli for specimens prepared with different combinations of water and foam contents were plotted. The mix combination that maximised the resilient modulus was considered the optimum combination.

To construct the contour line graphs of M40PA and M40LM, several mix combinations were made as shown in the test matrix in Figure 3.3. Tables 3.3 and 3.4 show the different test combinations that were carried out to develop the contour plots of M40PA and M40LM shown in Figures 3.4 and 3.5 (p.37).

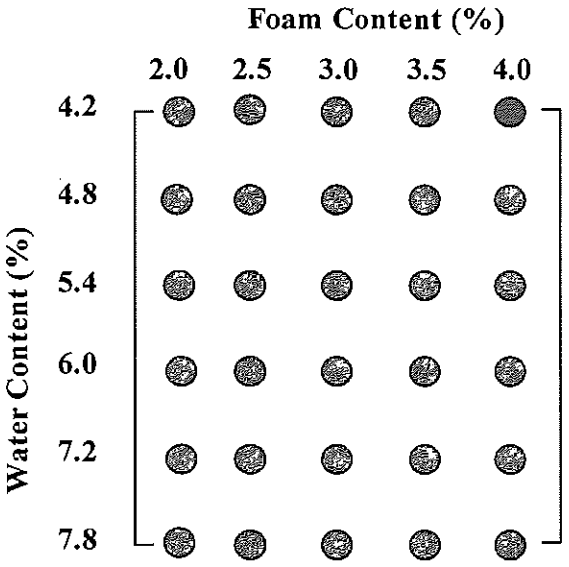

Figure 3.3 Test matrix for testing OMMC and OMFC of M40PA and M40LM mixes.

For M20PA and M20LM, a simplified approach, similar to that used in the first phase of the research to construct the contour line graphs for M20FA2C and M20FA, was employed. The contour line graphs for M20PA and M20LM are shown in Figures 3.6 and 3.7 (p.38). For easy reference and completeness, the contour line graphs for M20FA2C and M20FA are shown in Figures 3.8 and 3.9 (p.39), the details of which are in Transfund NZ Research Report No. 250 (Saleh & Herrington 2003, Figures 15.22 and 15.25 respectively).

Table 3.3 Resilient moduli (M_r) at different %MMC and %MFC for M40LM mix.

MMC (%)	MFC (%)	After 7 Days of Curing at Room Temperature, M_r (MPa)	Oven Dried, Ultimate M_r (MPa)
4.73	2.5	291.1	342.4
4.73	3.0	464.3	549.9
4.73	3.5	898.8	908.4
4.73	4.0	267.3	289.2
5.40	2.5	307.4	501.6
5.40	3.0	1009.8	1174.0
5.40	3.5	921.5	1186.4
5.40	4.0	485.7	771.6
6.75	2.5	1019.3	1108.7
6.75	3.0	1028.5	1805.5
6.75	3.5	1176.0	2150.0
6.75	4.0	917.5	1073.0
8.10	2.5	620.6	666.3
8.10	3.0	1056.5	1399.5
8.10	3.5	1515.0	1691.0
8.10	4.0	555.5	660.5

Table 3.4 Resilient moduli (M_r) at different %MMC and %MFC for M40PA mix.

MMC (%)	MFC (%)	After 7 Days of Curing at Room Temperature, M_r (MPa)	Oven Dried, Ultimate M_r (MPa)
4.73	2.5	149.4	179.4
4.73	3.0	226.5	284.0
4.73	3.5	190.0	286.4
4.73	4.0	307.3	309.7
5.40	2.5	301.8	367.6
5.40	3.0	384.4	394.0
5.40	3.5	344.8	504.1
5.40	4.0	585.9	637.1
6.75	2.5	383.6	714.8
6.75	3.0	524.7	790.3
6.75	3.5	674.9	987.4
6.75	4.0	491.2	899.5
8.10	2.5	276.9	282.0
8.10	3.0	366.4	541.6
8.10	3.5	632.3	765.6
8.10	4.0	393.8	579.4

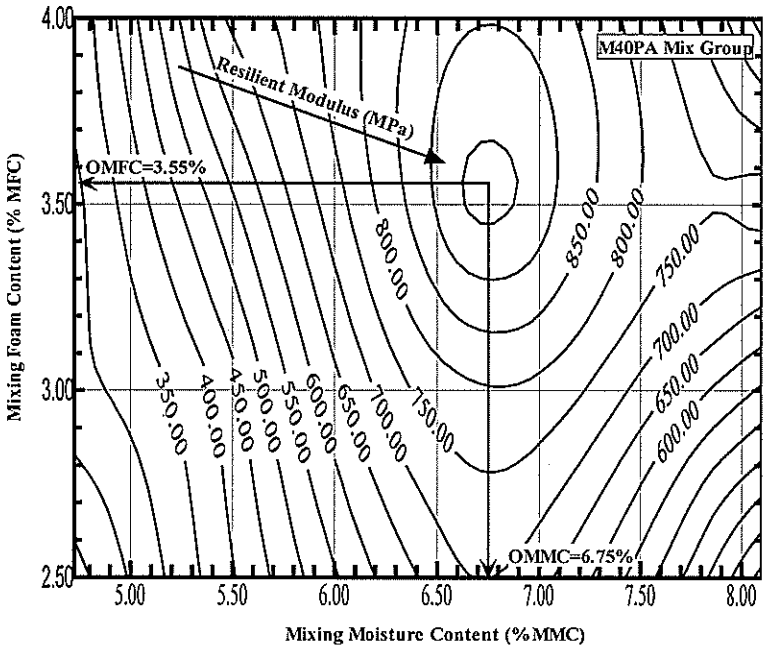

Figure 3.4 Determining the Optimum Mixing Moisture Content (OMMC%) and Optimum Mixing Foam Content (OMFC%) for M40PA.

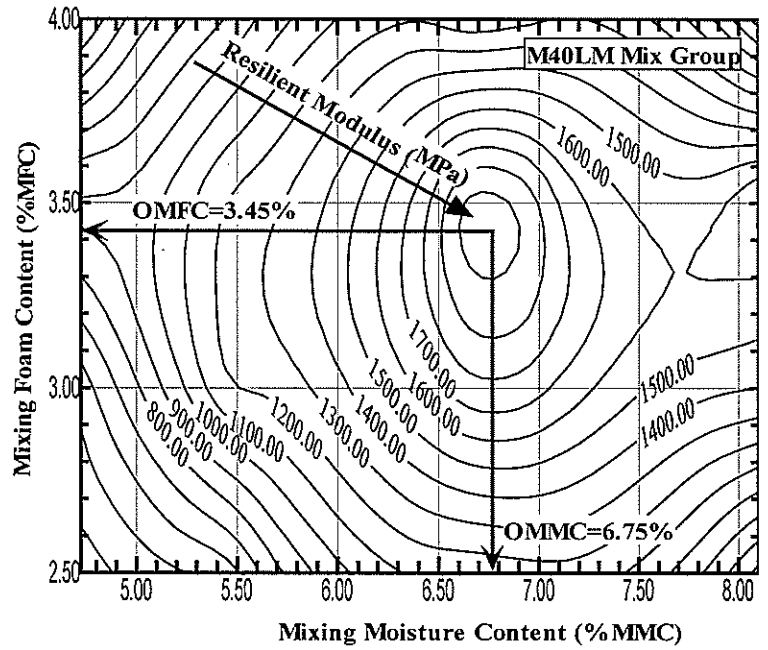

Figure 3.5 Determining the Optimum Mixing Moisture Content (OMMC%) and Optimum Mixing Foam Content (OMFC%) for M40LM mix.

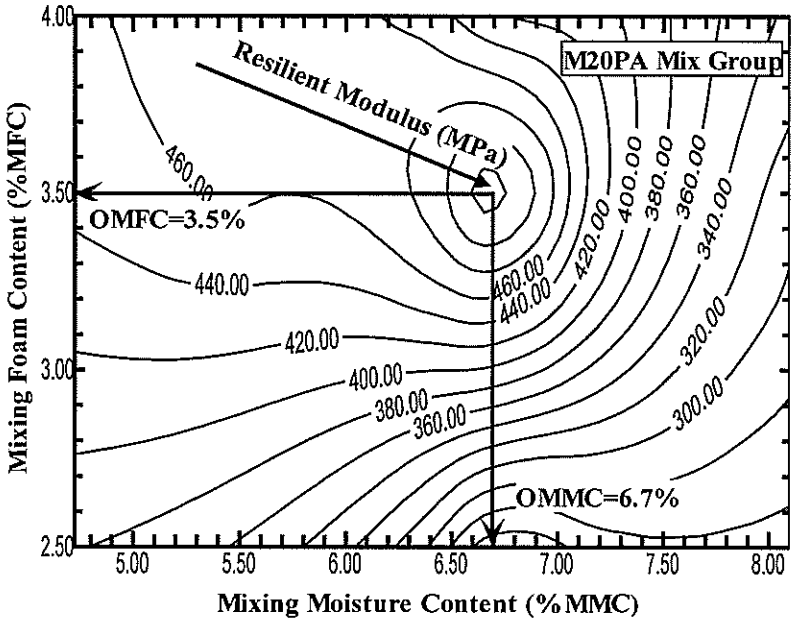

Figure 3.6 Determining the Optimum Mixing Moisture Content (OMMC%) and Optimum Mixing Foam Content (OMFC%) for M20PA mix.

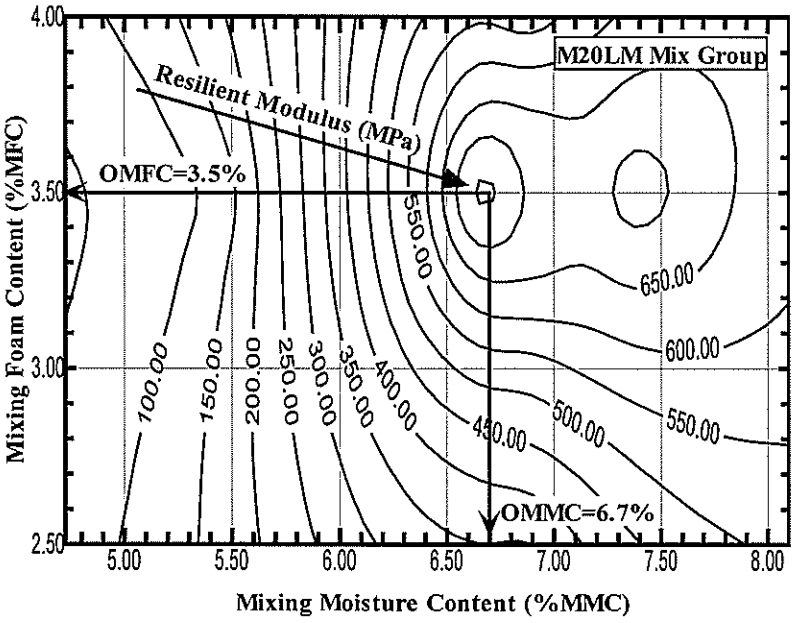

Figure 3.7 Determining the Optimum Mixing Moisture Content (OMMC%) and Optimum Mixing Foam Content (OMFC%) for M20LM mix.

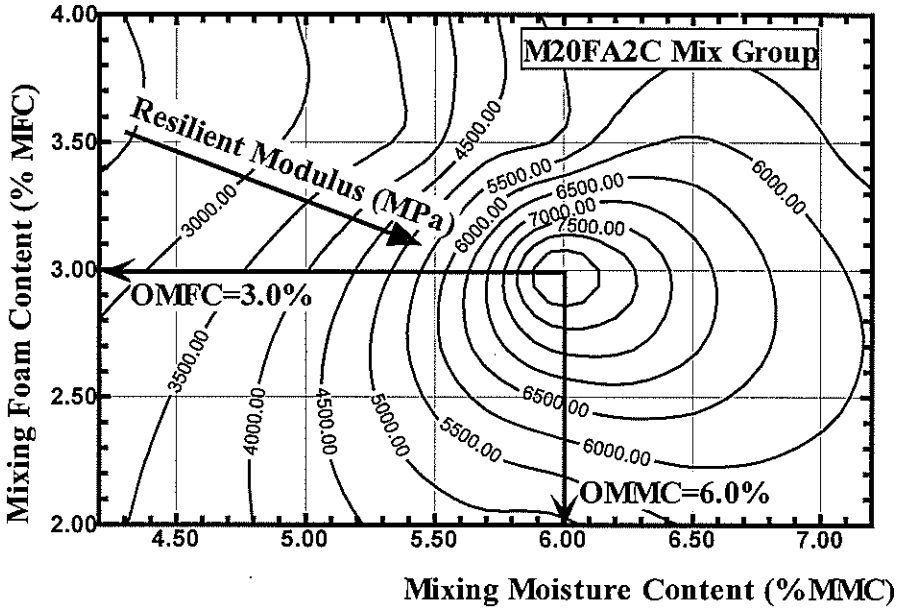

Figure 3.8 Determining the Optimum Mixing Moisture Content (OMMC%) and Optimum Mixing Foam Content (OMFC%) for M20FA2C mix (Saleh & Herrington 2003).

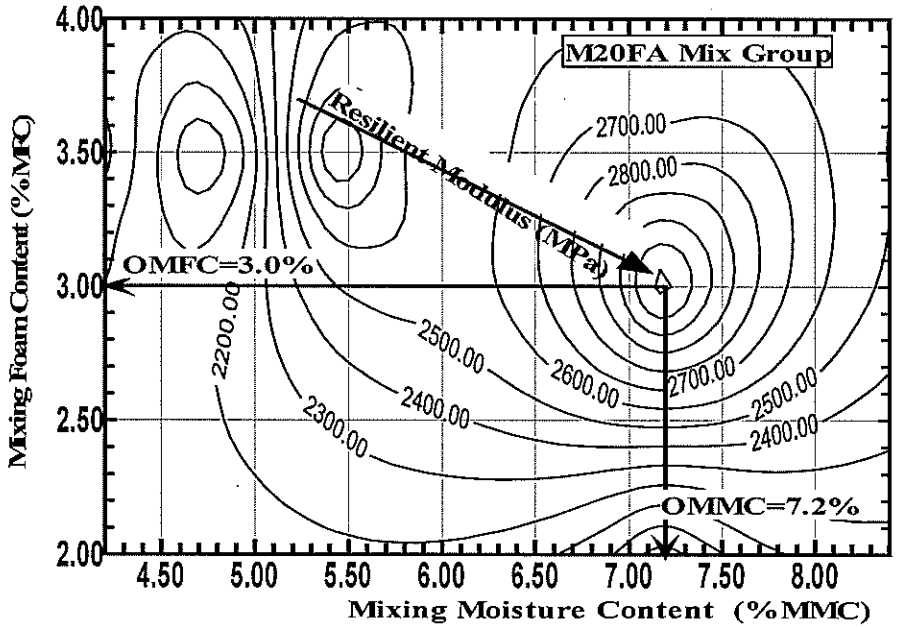

Figure 3.9 Determining the Optimum Mixing Moisture Content (OMMC%) and Optimum Mixing Foam Content (OMFC%) for M20FA mix (Saleh & Herrington 2003).

Table 3.5 contains the optimum mixing moisture and mixing foam contents together with the corresponding maximum resilient modulus for the different foam-stabilised mixes. The resilient modulus was measured at 19°C after 7 days of curing at room temperature.

Table 3.5 Mix design parameters for the six mix types.

Mix Type	Mix Design Parameters		
	OMMC (%)	OMFC (%)	Maximum M_r (MPa)
M40PA	6.75	3.55	1000
M40LM	6.75	3.45	2100
M20FA	7.2	3.0	3200
M20FA2C	6.0	3.0	8500
M20PA	6.7	3.5	520
M20LM	6.7	3.5	750

3.3 Effect of Aggregate Gradation and Mineral Fillers

It is clear from Table 3.5 that aggregate gradation and the type of mineral fillers have a significant effect on the resilient modulus and the optimum values of mixing foam and mixing moisture contents. For the same mineral fillers, the coarser gradation (AP-40) provides higher resilient modulus (M_r) values than the finer AP-20 mixes. This could be explained by the greater particle-to-particle contact that exists in the coarse aggregate gradation.

For the same gradation, adding hydrated lime has produced higher resilient modulus values as compared to adding Huntly pond ash. The reason for such high resilient modulus may be attributed to the cementitious reactions caused by lime. Using fly ash type C and Portland cement will also have a significant effect on the resilient modulus of foam-stabilised mixes. Later in this report, results are given of comparisons between other strength parameters such as indirect tensile strength and CBR for different gradations and mineral fillers that were carried out for the research.

4. Volumetric Properties of Foam-stabilised Mixes

The specific gravities of the coarse and fine aggregates were measured using the procedures given in ASTM C127 and ASTM C128. The specific gravity values of the mineral fillers were assumed. The voids and density relationships of the compacted mix were measured in accordance to AS 2891.8-1993. Table 4.1 lists the specific gravities and water absorption of the aggregates.

Table 4.1 Specific gravities (dry bulk, SSD bulk, apparent specific gravity) and water absorption (%) of aggregates used for foam-stabilised mixes.

Type of Aggregate	Dry Bulk sp G_{sb}	SSD Bulk sp G_{sb}	Apparent sp G_{sa}	Absorption (%)
Coarse	2.52	2.55	2.59	1.11
Fine	2.59	2.62	2.67	1.19
Fly ash type C	–	–	2.85	–

Notes: sp G_{sb} = Dry Bulk specific gravity of aggregates
sp G_{sa} = Apparent specific gravity of aggregates
SSD = Saturated Surface Dry condition

Table 4.2 contains the volumetric properties of M20FA and M20FA2C mixtures. The percentage of air voids is higher than that recommended in the hot mix asphalt (HMA) which ranges from 3.0% to 5.0%. The air voids of the specimens are about twice that of the HMA mix. Also the percentage of voids filled with bitumen is quite low (41.7 to 44.2%) compared to that of HMA (65 to 75%). The reason for this is the low bitumen content in these mixes (about 3.0%), compared to HMA which usually contains higher bitumen contents (5.0% to 5.5%). These findings agreed with the results reported by Lee (1981).

Table 4.2 Volumetric properties of foam-stabilised mixes.

Mix	Properties			
	G_{mb}	VMA (%)	VA (%)	VFB (%)
M20FA	2.26	15.0	8.4	44.2
M20FA2C	2.24	15.8	9.2	41.7

Notes: G_{mb} = Bulk specific gravity of the compacted mix
VMA = Voids in the mineral aggregates
VA = Air voids
VFB = Voids filled with bitumen

Premature cracking and/or ravelling are likely to occur with air voids of this magnitude because of oxidation of bitumen, and consequently the reduction of pavement durability.

The VMA values are about 15% and therefore Lee's (1981) finding is again validated. The percentage of voids in the mineral aggregates (VMA) is quite close to that used in the HMA for a mix of similar maximum nominal aggregate size.

5. Mechanical Properties of Foam-stabilised Mixes

After determining the optimum mixing moisture content (OMMC) and the optimum mixing foam content (OMFC) for the six mix types listed in Table 3.5, several specimens were prepared at these optimum values to test their mechanical properties. The properties that were analysed for these mixes are resilient modulus, temperature susceptibility, moisture susceptibility, indirect tensile strength, fracture energy, fatigue life, and CBR.

Different aggregate gradations, mineral filler types and sources of bitumen were used in this investigation. The effects of source and grade of the bitumens on these physical properties were evaluated as well.

5.1 Temperature Susceptibility

Six specimens for each of two mix types (M20FA and M20FA2C) were prepared at the optimum values of moisture (OMMC%) and foam contents (OMFC%) to evaluate the temperature susceptibilities of the stabilised mixes. The M20FA1C mixes were treated with foamed bitumens (produced from the eight bitumens that foamed well, excluding that from the Australian source) to investigate the effect of bitumen source on the mix properties. Both OMMC and OMFC were fixed (at the same %) regardless of the type of bitumen source.

Tables 5.1 and 5.2 contain the resilient moduli (M_r) at various temperatures of M20FA and M20FA2C specimens respectively, measured at different curing times. The fitted line equations that relate the resilient modulus and the testing temperature, and associated coefficients of determination (R^2 values) are also shown. The coefficients of determination values (R^2) are the indicators of the goodness of fit, and a fitted line is reliable when its R^2 value is close to one. Figures 5.1 and 5.2 depict the relationship between testing temperatures and resilient moduli at different curing times. The slope of this relationship expresses the temperature susceptibility of the mixes.

Table 5.1 Resilient moduli M_r (MPa) of M20FA at different curing times and testing temperatures.

Curing Time	Testing Temperature (°C)				Fitted Line Equation for M_r	R^2
	20	25	30	35		
Day 1	891.2	847.9	718.26	640.22	$M_r = -17.652*T + 1259.8$	0.9688
Day 3	2014.6	1462.0	1360.8	1073.4	$M_r = -58.496*T + 3086.3$	0.9186
Day 7	3277.6	2644.6	1979.4	1647.4	$M_r = -111.12*T + 5442.9$	0.9814
Dry	3431.4	2793.4	2259.4	1763.4	$M_r = -110.76*T + 5607.8$	0.9966

T = Temperature in °C

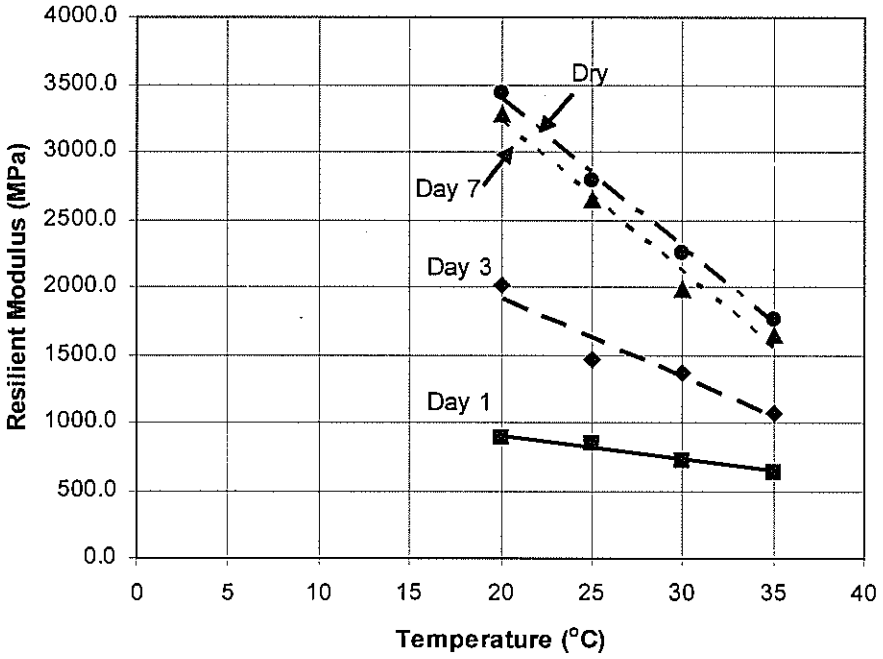

Figure 5.1 Temperature susceptibility of M20FA specimens for different curing periods.

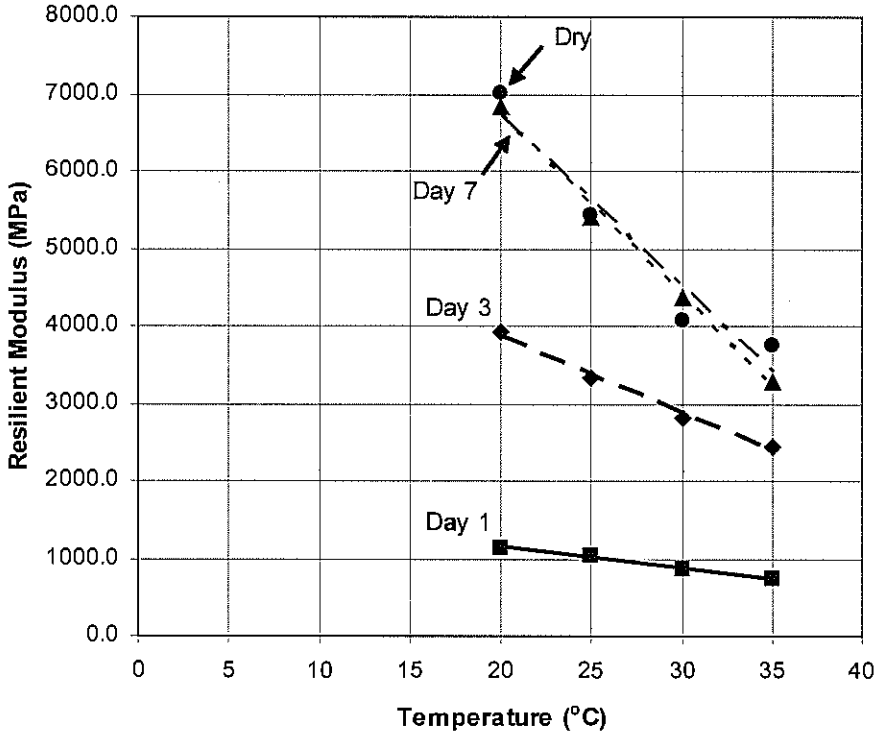

Figure 5.2 Temperature susceptibility of M20FA2C specimens for different curing periods.

Key : ■—— Day 1 ▲- - - Day 7
♦ _ _ . Day 3 ● ----- Dry

Table 5.2 Resilient moduli M_r (MPa) of M20FA2C at different curing times and testing temperatures.

Curing Time	Testing Temperature (°C)				Fitted Line Equation for M_r	R^2
	20	25	30	35		
Day 1	1143.0	1029.9	872.0	752.0	$M_r = -26.618*T + 1681.2$	0.996
Day 3	3922.0	3330.0	2825.0	2440.0	$M_r = -99.020*T + 5852.3$	0.991
Day 7	6830.8	5419.4	4382.6	3272.0	$M_r = -234.220*T + 11417$	0.995
Dry	7005.6	5423.6	4073.6	3764.8	$M_r = -221.450*T + 11157$	0.933

T = Temperature in °C

Both Figures 5.1 and 5.2 show the effects of both the curing period and testing temperature. Steeper slopes were obtained as the specimens experienced longer curing times. Also M20FA2C specimens have higher temperature susceptibility than M20FA specimens. This indicates that the type of mineral filler has an effect on the temperature susceptibility of the foam-stabilised mixes.

5.2 Moisture Susceptibility

In this test, six replicates were prepared for each of the three mix types M20FA, M20FA2C, M20FA1C. Each of the six replicates were subdivided into two subgroups (each subgroup has three replicates) with approximately the same average percentage of air voids. The resilient moduli of all replicates were measured on the dry basis at 25°C testing temperature. The average of these values for M20FA, M20FA2C and M20FA1C is shown in Table 5.3.

Table 5.3 Resilient moduli (M_r) and Index of Retained Strength (IRS) of foam-stabilised mixes M20FA, M20FA2C, M20FA1C, soaked for up to 5 days.

M20FA						
Period of soaking (hours)	24	48	72	96	120	**Ultimate M_r (MPa)**
Soaked resilient modulus (MPa)	2523.0	2277.3	2476.0	3100.7	2483.7	
Index of Retained Strength (%)	91	82	89	112	89	**2776.7**
M20FA2C						
Period of soaking (hours)	24	48	72	96	120	**Ultimate M_r (MPa)**
Soaked resilient modulus (MPa)	4705.7	6032.7	4365.0	4273.3	4215.3	
Index of Retained Strength (%)	73	93	68	66	65	**6455**
M20FA1C						
Period of soaking (hours)	24	48	72	96	120	**Ultimate M_r (MPa)**
Soaked resilient modulus (MPa)	5195.5	5397.0	5412.5	4769.0	5142.0	
Index of Retained Strength (%)	96	99	100	88	95	**5437.5**

These resilient moduli were considered the ultimate resilient moduli for these mixes because the measurements were done on the dry basis. Half the specimens were then immersed for five days in a temperature-controlled water bath at 25°C and the resilient moduli were determined at 24-hour intervals. Each value of soaked modulus was then divided by the ultimate modulus to obtain the Index of Retained Strength (IRS), which expresses the resistance of that mixture to moisture. Table 5.3 lists the resilient moduli and IRS values of the soaked M20FA and M20FA2C and M20FA1C specimens. Figure 5.3 depicts the relationship between the IRS values and duration of soaking.

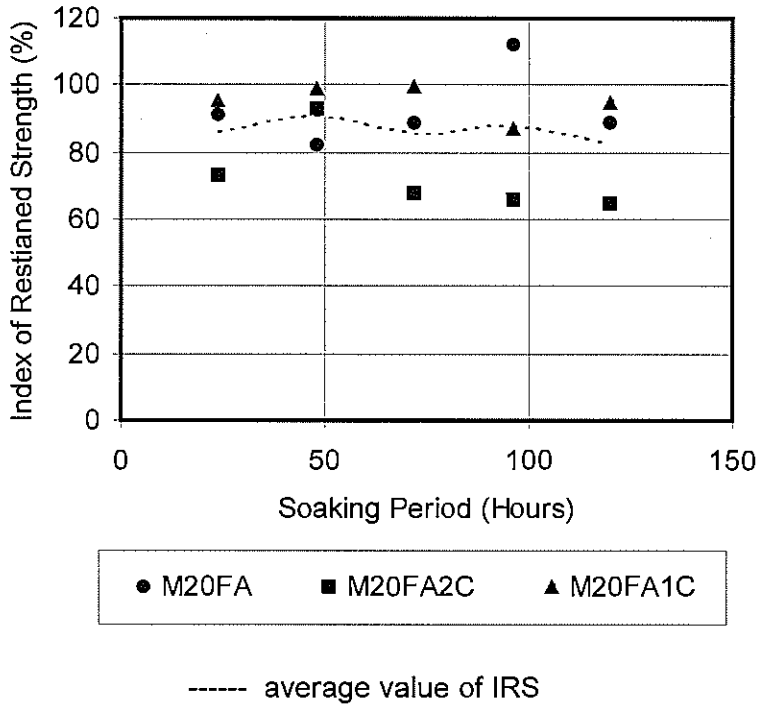

Figure 5.3 Moisture susceptibility of foam-stabilised mixes as a relationship between soaking period and IRS.

Figure 5.3 shows a similar trend in all the three mix types with an average value of the IRS about 86% as shown by the dotted line. It is clear that the foam-stabilised mixes were showing excellent moisture resistance as the mixes kept their integrity and strength and they did not deteriorate significantly, even after 5 days of continuous soaking in water. This behaviour also indicates that the foamed bitumen possesses good adhesion, and the foamed bitumen does not strip after soaking in water.

The average IRS value of 86% is reasonably high and comparable with that of the HMA mixes. The Australian Provisional Guide for Selection and Design of Asphalt Mixes (APRG 2002) states that a minimum IRS value of 80% is used in a number of specifications for the acceptance of an asphalt mix having a satisfactory resistance to moisture.

5.3 Effect of Bitumen Source and Grade

The purpose of this section is to evaluate the effect of bitumen source and penetration grade on both temperature and moisture susceptibilities of foam-stabilised mixes.

5.3.1 Effect of Source and Grade on Temperature Susceptibility

Table 5.4 lists the resilient modulus values of M20FA1C specimens measured at different temperatures. Figure 5.4 shows comparisons between the different mixes. In correlation with results in Section 1.4 (Table 1.4 and Figure 1.2, temperature susceptibility of bitumen), the PVN approach closely corresponds to the temperature susceptibility properties of foamed bitumen mixtures.

Table 5.4 Resilient moduli M_r (in MPa) of M20FA1C specimens produced from the eight bitumen types, at different temperatures.

Bitumen Type	Resilient Modulus M_r (MPa)					
	20 °C	25 °C	30°C	35°C	Fitted Line Equation for M_r	R^2
SHL80	6335	4731	3697	2634	$M_r = -247*T + 11141$	0.99
SHL180	7771	5866	4618	3068	$M_r = -310*T + 13860$	0.99
VEN80	5121	4274	3557	3041	$M_r = -141.6*T + 7891$	0.99
VEN180	4324	3522	2765	2024	$M_r = -153.6*T + 7383$	1.00
DLT80	8539	6460	5048	3468	$M_r = -336.5*T + 15133$	0.99
AR2000	4606	3626	2374	1767	$M_r = -197.8*T + 8532$	0.98
AR4000-1	8616	5909	4311	3189	$M_r = -369.5*T + 15669$	0.96
AR4000-2	4427	3547	2596	2011	$M_r = -166*T + 7710$	0.99

T = Temperature in °C

C170 was not analysed further as it was unsuitable for foam production.

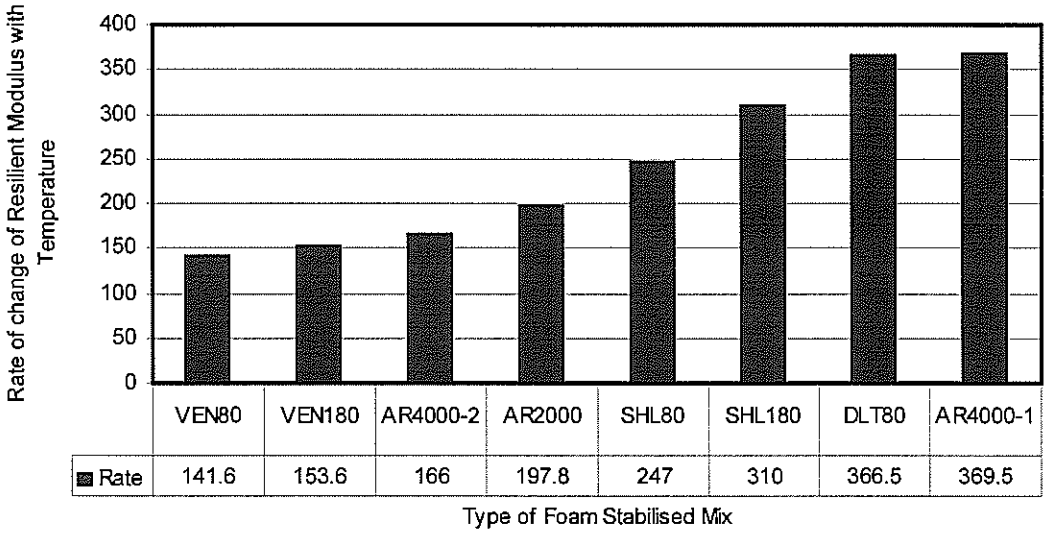

Figure 5.4 Temperature susceptibility of M20FA1C specimens of the eight bitumen types, shown by rate of change of M_r with temperature.

The VEN80 and VEN180 bitumens were classified as yielding the least temperature-susceptible bitumens (Figure 1.2) and their foamed stabilised mixes showed the least temperature-susceptible mixes, as shown in Figure 5.4. However, there are still some discrepancies. One example is AR-2000, which was classified as one of the most temperature-susceptible binders (Figures 1.1 to 1.3), yet it yielded mixtures that were not very temperature-susceptible as shown in Figure 5.4.

5.3.2 Effect of Source and Grade on Moisture Susceptibility

Table 5.5 lists the resilient moduli and index of retained strength (IRS) values. The IRS is defined as the percentage of the resilient modulus after soaking to the resilient modulus value before soaking. To measure the IRS values, the resilient moduli of the dry specimens were first measured, and then specimens were subjected to five days soaking. The resilient moduli were measured every 24 hours. Figure 5.5 shows the IRS values for the eight different types of bitumen over different soaking periods. AR4000-1 shows the highest IRS values while AR4000-2 provides the lowest IRS values. The average IRS value for all types over the five days soaking period exceeded 90%, which is an excellent value.

Table 5.5 Resilient moduli M_r (in MPa) and IRS values of soaked M20FA1C specimens produced from the eight bitumen types, over 5 days.

Bitumen Type		Soaking Period (hours)					
		0	24	48	72	96	120
SHL80	M_r	4662	4756	3786	5370	4199	4333
	IRS	100.00	102.0	81.2	115.2	90.1	92.9
SHL180	M_r	5438	5196	5397	5413	4769	5142
	IRS	100.0	95.5	99.3	99.5	87.7	94.6
VEN80	M_r	5308	4800	4778	5008	4589	4582
	IRS	100.0	90.4	90.0	94.4	86.5	86.3
VEN180	M_r	3564	3443	2993	3242	3024	2884
	IRS	100.0	96.6	84.0	91.0	84.8	80.9
DLT80	M_r	7215	5637	5606	5115	5557	5519
	IRS	100.0	78.1	77.7	70.9	77.0	76.5
AR2000	M_r	3435	3300	3124	4253	3707	3813
	IRS	100.0	96.1	90.9	123.8	107.9	111.0
AR4000-1	M_r	5772	6371	5958	7876	6902	7100
	IRS	100.0	110.4	103.2	136.5	119.6	123.0
AR4000-2	M_r	4528	3877	2948	3383	3046	4200
	IRS	100.0	85.6	65.1	74.7	67.3	92.8

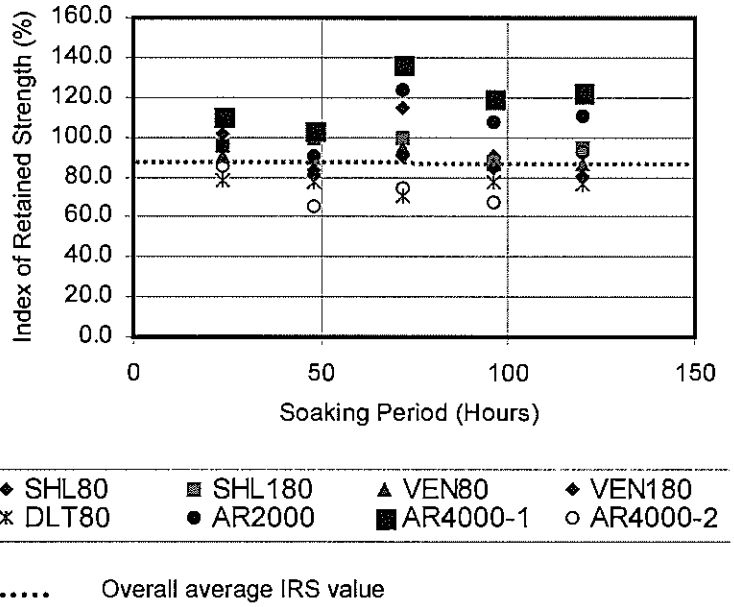

Figure 5.5 Moisture susceptibility of M20FA1C specimens produced from the eight bitumen types, showing effect of soaking on IRS values, and the average IRS value.

Figure 5.5 shows no exact pattern concerning the susceptibility of the specimens to moisture. Instead, a scattered pattern was found for different soaking periods.

5.4 Temperature Susceptibilities of Foam-stabilised & HMA Mixes

The resilient modulus test was also carried out on another mix, an AC10 dense-graded HMA (hot mix asphalt) produced from SHL80. Despite the fact that AC10 is a surface course material, it has been used to provide a comparison with the behaviour of the foam-stabilised materials because it has been used for a long time and its performance is well known. The AC10 mix was secured from one of the local suppliers.

The resilient modulus test was conducted on it at 15°, 20°, and 25°C. The maximum temperature of the test was limited to 25°C so that the HMA specimen was kept in the desired temperature and loading range within which it will retain its elastic behaviour. Table 5.6 contains the results of the resilient modulus at different temperatures and the fitted equation for the resilient modulus and temperature. Figure 5.6 shows a comparison between the AC10 HMA and the foam-stabilised mix (M20FA1C) produced from the same source and grade of bitumen.

Clearly the resilient modulus of the HMA undergoes a decrease at elevated temperatures while the foam-stabilised mix still maintains high resilient modulus value. This finding agrees with Bissada (1987). Muthen (1999) attributes the high resilient modulus values of foam-stabilised mixtures at high temperatures to the preservation of the friction between the larger particles because they are not coated with binder, even though the bitumen–fines mortar in a foamed bitumen mixture will

soften with increasing temperature. In addition, HMA contains a high bitumen content (about 5.5%) compared to the foam-stabilised mixes, which usually contain only up to 3.0 to 3.5% binder content. This high bitumen content will cause the HMA to be more temperature-susceptible compared to foam-stabilised mixes.

This indicates that foam-stabilised mixes are likely to suffer much less distortion and rutting compared to the HMA in areas where the pavement temperature is expected to be quite high on hot summer days.

Table 5.6 Resilient Modulus (M_r) for AC10 dense graded hot mix asphalt, for comparison with foam-stabilised mix (M20FA1C) (Figure 5.6).

Temperature (°C)	15	20	25	Fitted Equation for M_r	R^2
Resilient Modulus (MPa)	5399	3409	2094	$M_r = 10356.5 - 366*T$	99

T = Temperature in °C

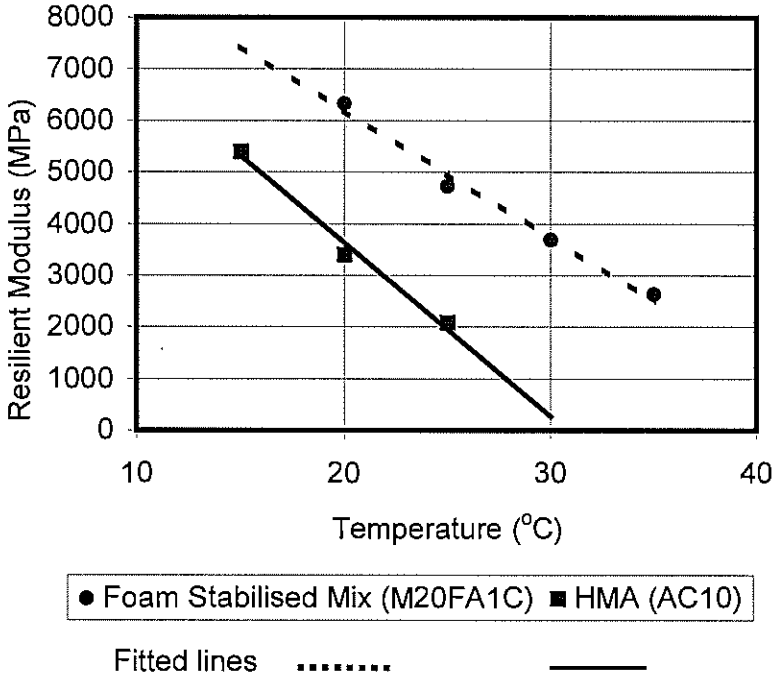

Figure 5.6 Comparison between the temperature susceptibilities of M20FA1C foam-stabilised mix and dense-graded AC10 HMA.

5.5 Indirect Tensile Strength (ITS)

The ITS was determined using the Humboldt Master Loader HM-3000 shown in Figure 5.7, in accordance with NZS 3112:Part 2:1986 with a loading speed of 50.8 mm/min.

The specimens were placed in the loading frame and aligned to ensure that the axis of symmetry and direction of loading act through the centroid of the specimens. The ITS of the mixtures was obtained using the following equation.

$$ITS = \sigma_{x\,max} = \frac{2 * P_{max}}{\pi * d * t} \times 1000 \qquad \text{Equation 6}$$

where:

ITS	=	indirect tensile strength (kPa)
σ_{xmax}	=	maximum horizontal tensile stress (kPa)
P_{max}	=	maximum applied force or load (N)
d	=	diameter (mm)
t	=	specimen height (mm)

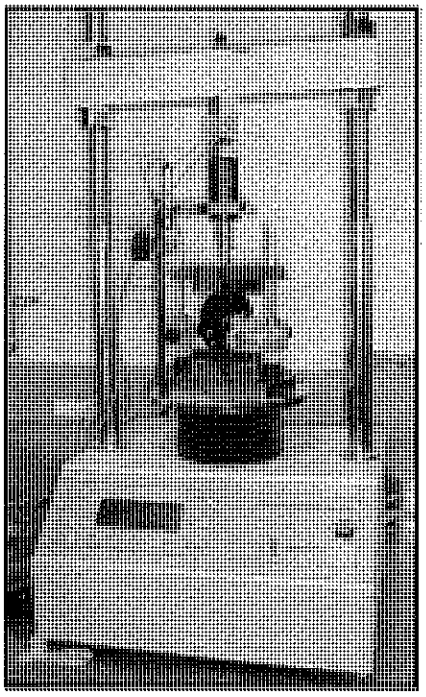

Figure 5.7 Humboldt Master Loader HM-3000, used for measuring ITS.

The ITS test was carried out for the foam-stabilised specimens with different gradations and mineral fillers, and for the AC10 HMA. Table 5.7 contains the ITS results for these different foam-stabilised mixes together with those for AC10 HMA. Figure 5.8 depicts the ITS results for different mixes made of different aggregate gradations (AP-40 and AP-20) and different types of mineral fillers (see Section 3.1, Table 3.1). The effect of gradation and type of mineral fillers on the ITS is quite clear as shown in Figure 5.8. Foam-stabilised mixes with Huntly pond ash as a mineral filler showed the lowest ITS value while those containing fly ash type C and fly ash type C with 1% or 2% cement showed a significant increase in ITS values.

The ITS value for the AC10 HMA is about 3 times the highest ITS value for foam-stabilised mixes. This indicates that fatigue performance of the AC10 HMA is likely to be much better than that expected from the foam-stabilised mixes. This can be attributed to the higher binder content in the HMA compared to that in the foam-stabilised mixes.

Table 5.7 Indirect Tensile Strength (ITS) of the foam-stabilised mixes and AC10 HMA.

Mix type	Indirect Tensile Strength, ITS (kPa)
M20LM	142
M20PA	72
M40LM	153.5
M40PA	63
M20FA	359
M20FA1C	378
M20FA2C	388
AC10 HMA	1198

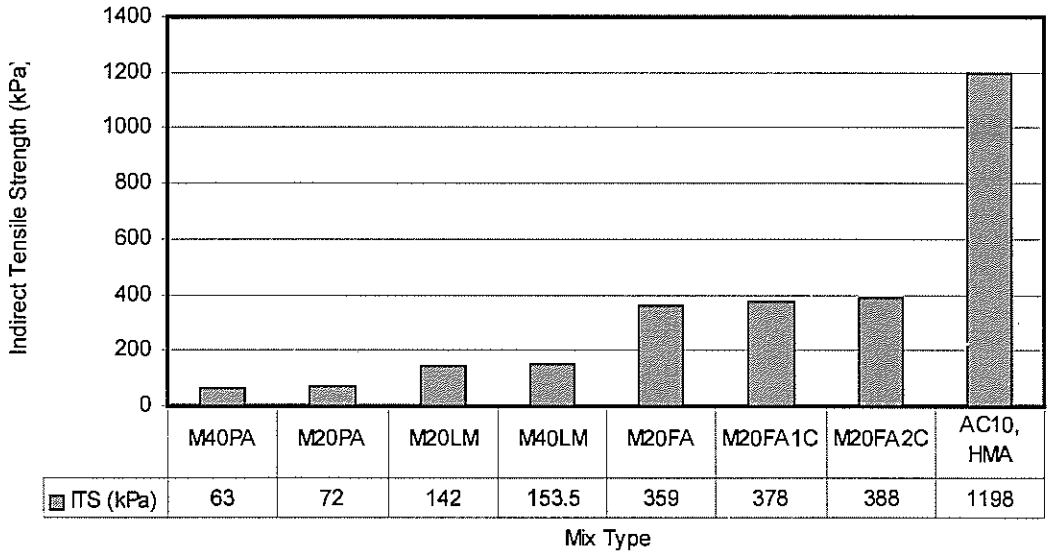

Figure 5.8 Comparison of ITS for different foam-stabilised mixes and AC10 HMA.

5.6 Fracture Energy

The fracture energy of foam-stabilised mixes was computed by calculating the area under the force displacement curve as shown in Figure 5.9. This parameter is highly correlated to the fatigue life of the mix. Figure 5.10 shows a comparison between the force displacement curves of the AC10 HMA and M20FA1C foam-stabilised mix. It is clear from this graph that the fracture energy of the HMA is much higher than that of the foam-stabilised mixes. In addition, the AC10 HMA shows much more flexibility than the foam-stabilised mixes since the amount of deformation before failure for the HMA is much higher than that for the foam-stabilised mix.

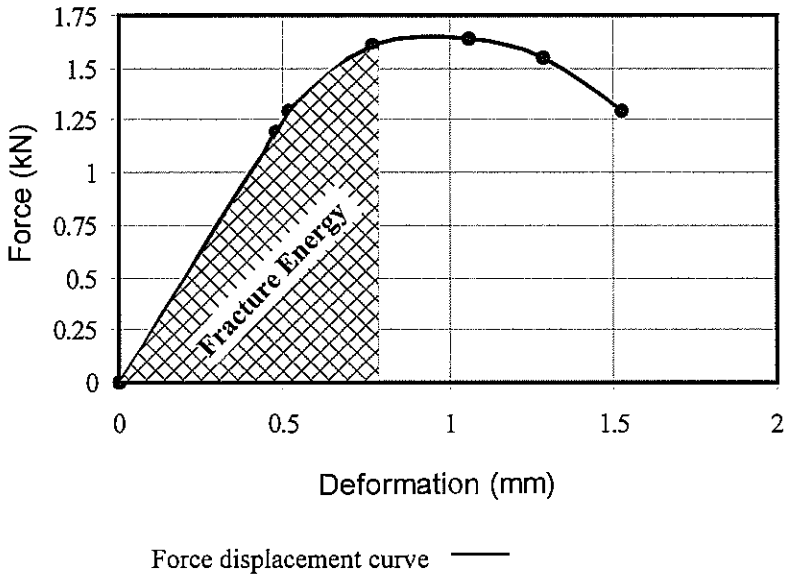

Figure 5.9 Definition of fracture energy for foam-stabilised mixes.

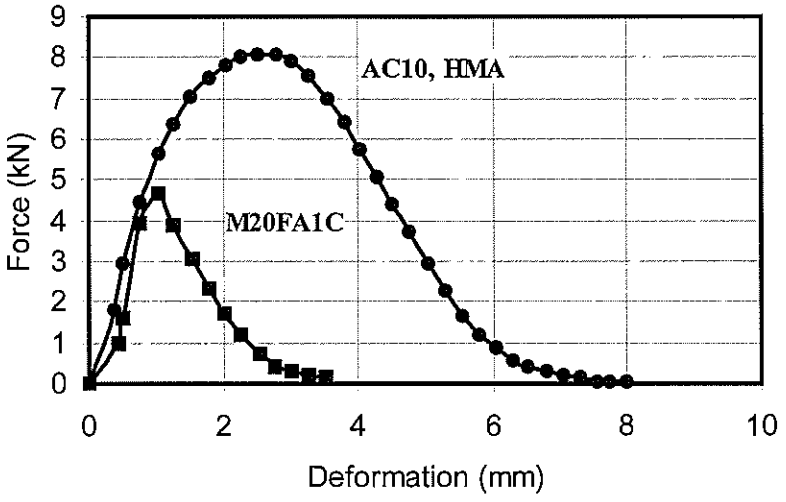

Figure 5.10 Comparison between fracture energy for M20FA1C foam-stabilised mix and AC10 HMA.

To study the viscoelastic behaviour of the foam-stabilised mixes, the indirect tensile strength test was conducted at two rates of loading: 50.8 mm/min and 1 mm/min. The results of this test are given in Table 5.8. Figure 5.11 shows the relationship between the horizontal tensile stress and the corresponding horizontal tensile strain for M20FA2C mixes at these two different rates of loading.

The effect of loading rate is remarkable as the fracture energy for the slow loading rate is much less than that for the faster loading rate. The energy required to break the M20FA2C loaded at 1 mm/min is 0.43 kN.mm, while the energy required to break specimens from the same mix loaded at 50.8 mm/min is 1.39 kN.mm. This indicates that foam-stabilised mixes are viscoelastic materials. Furthermore, the

results of the fracture energy shown in Table 5.8 indicate that the HMA mixture will give superior performance in fatigue (i.e higher fatigue life), compared to the foam-stabilised mixes, because of its high fracture energy.

Table 5.8 Fracture energy of foam-stabilised mixes and HMA at different loading rates.

Mix Type	Fracture Energy (kN.mm)	
	Rate of loading	
	1 mm/min	50.8 mm/min
M20FA	0.47	1.48
M20FA1C	0.47	1.68
M20FA2C	0.43	1.39
AC10-HMA	4.91	13.87

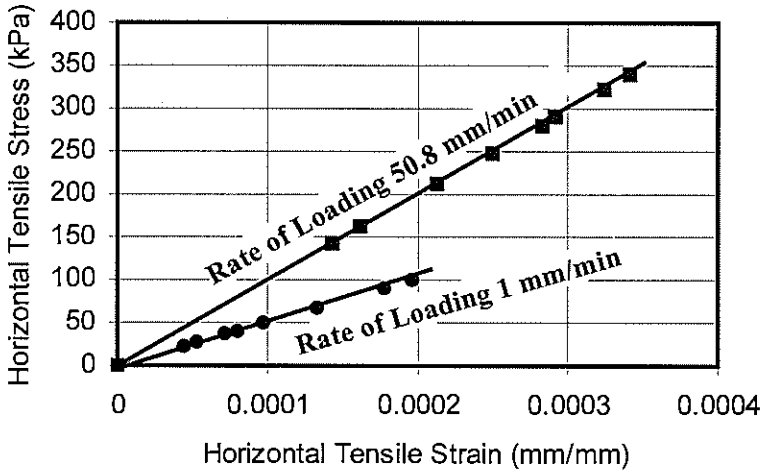

Figure 5.11 Effect of two rates of loading on foam-stabilised mixes.

5.7 Fatigue Life

The use of foam bitumen to stabilise unbound granular materials will transform these materials to bound materials. Also because of the high stiffness values for these mixes, they are likely to arrest high stress concentrations, therefore fatigue cracking will be a significant form of distress in these materials. The Nottingham indirect fatigue test was used to measure the fatigue life of foam-stabilised mixes (Read & Brown 1996).

The specimen is loaded diametrically with a vertical compressive force as shown in Figure 5.12. This indirectly generates a tensile stress across the vertical diameter. For any stress level specified by the operator, the magnitude of the applied compressive force and the corresponding horizontal tensile strain can be calculated by the following equations.

$$P = \frac{\sigma_{x\max} * \pi * d * t}{2} \qquad \text{Equation 7}$$

$$\varepsilon_{x\max} = \frac{\sigma_{x\max}}{S_m}(1 + 3 * \nu) * 1000 \qquad \text{Equation 8}$$

where:

P	=	Vertical compressive force (kN)
$\sigma_{x\max}$	=	Maximum horizontal tensile stress (kPa)
$\varepsilon_{x\max}$	=	Maximum horizontal tensile strain (με)
ν	=	Poisson's ratio
d	=	Diameter of the specimen (m)
t	=	Thickness of the specimen (m)
S_m	=	Stiffness modulus (resilient modulus) of the specimen (MPa)

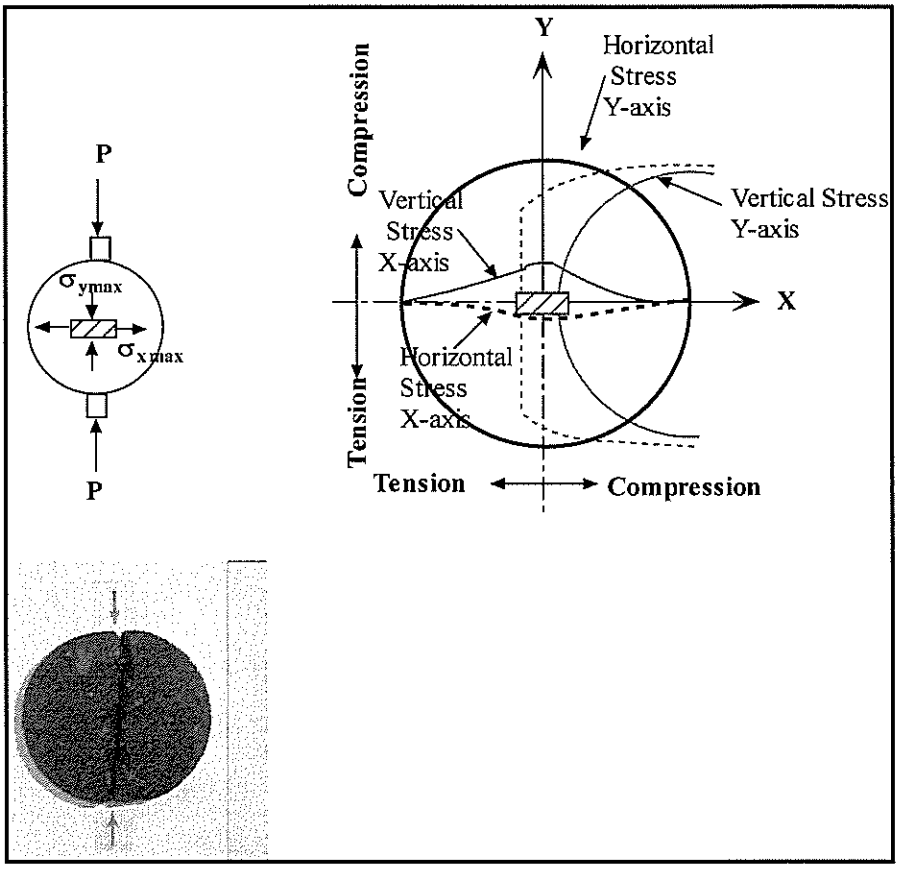

Figure 5.12 Stress distribution in the indirect tensile fatigue test (ITFT) loading of specimen.

Upper left: Frontal view of specimen undergoing Indirect Tensile loading ($\sigma_{y\,max}$ = maximum vertical compressive stress).

Lower left: HMA specimen (100 mm-diameter x 40 mm-thick) showing direct *s*plit caused by horizontal tensile strains.

In order to produce a fatigue relationship for a particular material, a number of identical specimens need to be obtained. The stiffness modulus (resilient modulus) values of these specimens are tested first so that the horizontal tensile strain developed at the centre of the test specimen during the fatigue test can be calculated. The size of the test specimen is important because the value of the applied stress (σ_{xmax}) and therefore the generated horizontal tensile strain is dependent upon it.

The preferred geometry for the indirect tensile fatigue test (ITFT) is a 100 mm-diameter and 40 mm-thick specimen (Read & Brown 1996). With such dimensions, to generate a horizontal tensile stress of 600 kPa, a force of about 4.3 kN has to be applied on the specimen. This is within the capacity of the loading frame (about 5 kN) of the UTM[3] machine available at the University of Canterbury.

The failure is defined to have occurred when either of the following two cases occurs first:

1. A direct split of the specimen (as shown in Figure 5.12), or
2. The vertical deformation reaches 9 mm, as defined by Read & Brown (1996).

To obtain a fatigue life curve, the normal procedure is to test the first specimen at the maximum achievable horizontal stress level, and then test the subsequent specimens at lower stresses.

Once all testing is complete, the horizontal tensile strain generated at the centre of the specimens is calculated from Equation 8. The initial horizontal tensile strain is then plotted versus the number of load repetitions to failure on a log-log graph. This relationship can then be compared with fatigue relationships of known materials to evaluate the relative performance.

In this research, the indirect tensile fatigue test was carried out on dense-graded AC10 HMA, open-graded porous asphalt (OGPA), and foam-stabilised mix (M20FA1C). Both the AC10 HMA and the OGPA were taken from a local supplier in Christchurch.

Two sets of fatigue models were developed for the three mixes used, and are shown by equations 9 and 10.

$$N_f = a * \varepsilon^b \qquad \text{Equation 9}$$

$$N_f = \alpha * \varepsilon^{\beta} * M_r^{\gamma} \qquad \text{Equation 10}$$

where:

N_f = Number of load repetitions to failure
ε = Initial horizontal tensile strain in mm/mm
M_r = Resilient modulus in MPa
a, b, α, β, and γ = regression constants depending on the material type

5.7.1 Fatigue Models for AC10 Dense-Graded HMA

Equations 11 and 12 are the fatigue equations developed for dense-graded HMA at the University of Canterbury Transportation Laboratory. Figures 5.13 and 5.14 compare the predicted and measured numbers of load repetitions. The coefficient of determination (R^2) for both models is very close to 1 (one), which means that these models explain at least 99% of the variability of the data. Although Equation 12 explicitly accounts for the effect of the resilient modulus, Equation 11 however implicitly accounts for the effect of the modulus because the modulus value will affect the generated tensile strains.

[3] UTM = Universal Testing Machine.

$$N_f = 2.35*10^{-13} * \varepsilon^{-4.719} \qquad \text{Equation 11}$$
$$R^2 = 0.996$$

$$N_f = 6.64*10^{-11} * \varepsilon^{-4.5144} * M_r^{-0.5116} \qquad \text{Equation 12}$$
$$R^2 = 0.995$$

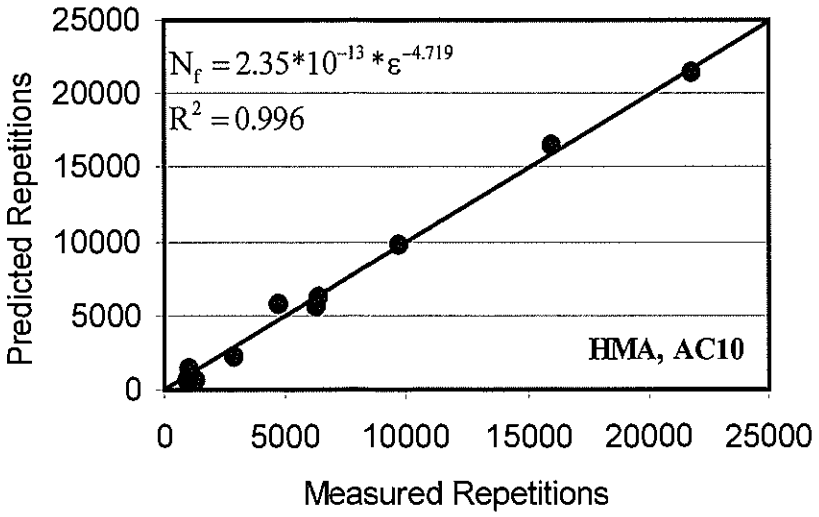

Figure 5.13 Predicted versus measured number of load repetitions for fatigue models for AC10 HMA using equation 11 model.

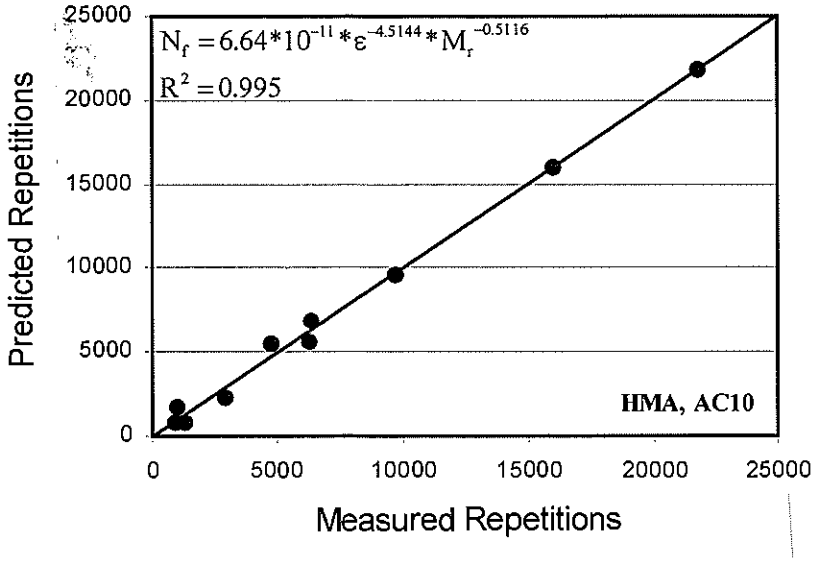

Figure 5.14 Predicted versus measured number of load repetitions for fatigue models for AC10 HMA using equation 12 model.

Figure 5.15 shows a comparison between the University of Canterbury (UC) fatigue model and BRRC (Belgian Road Research Centre), TRRL (Transport Road Research Laboratory, UK), PDMAP (Probabilistic Distress Model for Asphalt Pavement,

USA), and the Austroads fatigue model. It should be noted that the BRRC, TRRL and Austroads are field fatigue models. In other words, these models have been calibrated by using shift factors to adjust the laboratory models to match the field performance. The fatigue curve shown for the PDMAP is for the laboratory fatigue model without any field calibrations. The UC model is reasonably close to both BRRC and PDMAP fatigue models.

The difference among the three models could be related to the difference in the materials tested or the laboratory test method. There is a shift factor of up to 30 between the TRRL fatigue model and the UC model, and of up to 100 between the Austroads and UC models. This is due to field calibration adjustment and probably to the difference in the material properties, or both. The UC fatigue model for dense-graded HMA needs field calibration to adjust it to New Zealand field conditions. A close look to Figure 5.15 clearly shows the significant difference between the fatigue life predicted by the different models, therefore New Zealand should develop its own fatigue models that cover a wide band of materials (AC-14, AC20,... etc.) for different types of binders (polymer modified or conventional binders) which suit its materials, climate, and traffic loading.

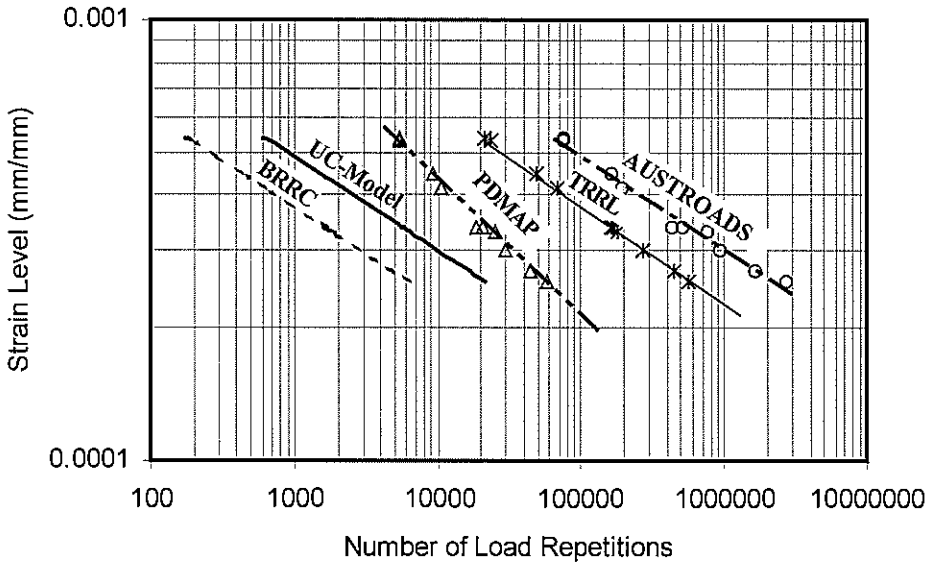

Figure 5.15 Comparison between University of Canterbury fatigue model (UC-Model) and other fatigue models for HMA.

5.7.2 Fatigue Models for Open-Graded Porous Asphalt (OGPA)

Equations 13 and 14 show the fatigue models developed for open-graded porous asphalt (OGPA). Figures 5.16 and 5.17 show the measured versus predicted number of load repetitions for both models shown by Equations 13 and 14. Both models reasonably predict the number of load repetitions to failure.

$$N_f = 6.31 * 10^{-5} * \varepsilon^{-2.18143}$$
$$R^2 = 0.93$$

Equation 13

$$N_f = 1.21*10^{-9} * \varepsilon^{-2.56} * M_r^{1.0704}$$
$$R^2 = 0.903$$

Equation 14

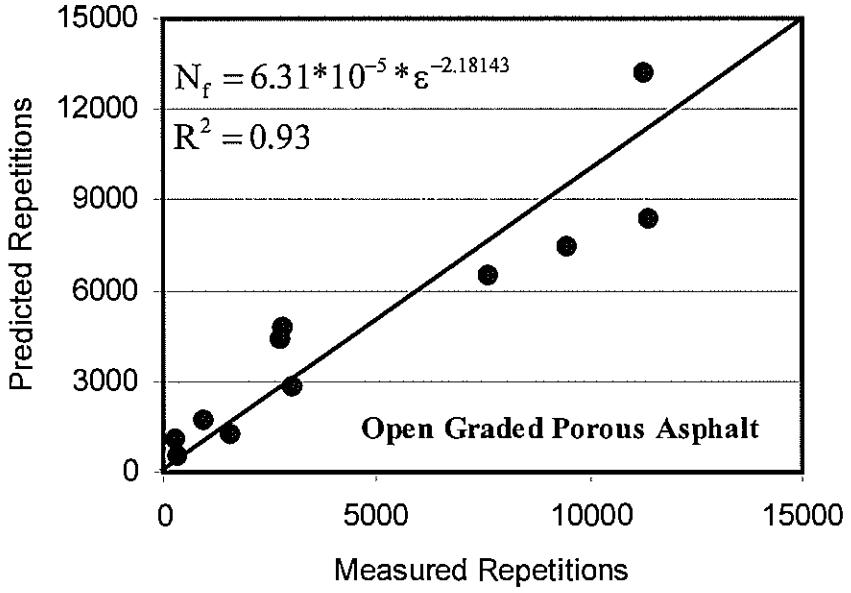

Figure 5.16 Predicted versus measured number of load repetitions for open-graded porous asphalt using equation 13 model.

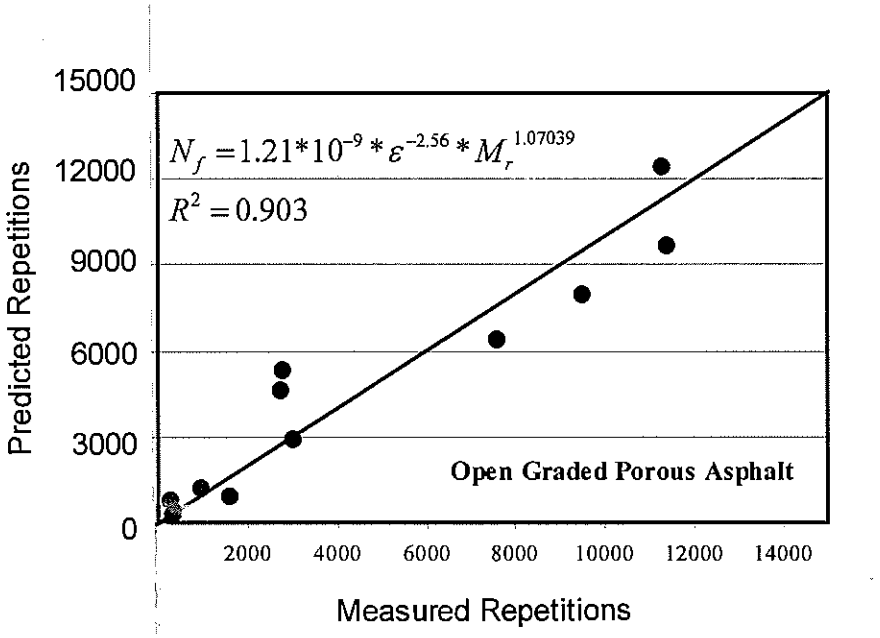

Figure 5.17 Predicted versus measured number of load repetitions for open-graded porous asphalt using equation 14 model.

5.7.3 Fatigue Models for Foamed Bitumen-Stabilised Mixes

Equations 15 and 16 are the two forms of fatigue models developed for M20FA1C mixes. Figure 5.18 illustrates the goodness of fit of the model shown in Equation 16. Figure 5.19 shows a comparison between the fatigue life of AC10 HMA, open-graded porous asphalt (OGPA) and foam-stabilised mix M20FA1C. It is obvious that HMA has a much higher fatigue life compared to foam-stabilised mixes when they are compared at the same tensile strain level. This finding agrees with the indirect tensile strength values and fracture energy discussed in Sections 5.5 and 5.6. The high fatigue life of the HMA can be attributed to the high binder content, and the good homogeneous coating of bitumen on all aggregate particles that provide flexibility to the mix.

In Figure 5.19, the slopes of the fatigue curves of the OGPA and the foam-stabilised mixes are steeper than that of the HMA. This clearly indicates that the fatigue performance of these mixes is inferior to that of the HMA mixes.

In the design of the foam-stabilised mixes, the optimum foam and water content were determined so that the resilient modulus of the mix will be maximised with no regard for fatigue life. Therefore, it is recommended to include some parameters such as indirect tensile strength or fracture energy in the mix design procedure. Thus, the foam, water content, and the ratio between foam and mineral fillers content should be determined to optimise the value of ITS or fracture energy. This will ensure longer fatigue life for these mixes.

$$N_f = 7.67 * 10^{-3} * \varepsilon^{-1.2207} \qquad \text{Equation 15}$$
$$R^2 = 0.979$$

$$N_f = 0.3208 * \varepsilon^{-2.525} * M_r^{-1.9256} \qquad \text{Equation 16}$$
$$R^2 = 0.996$$

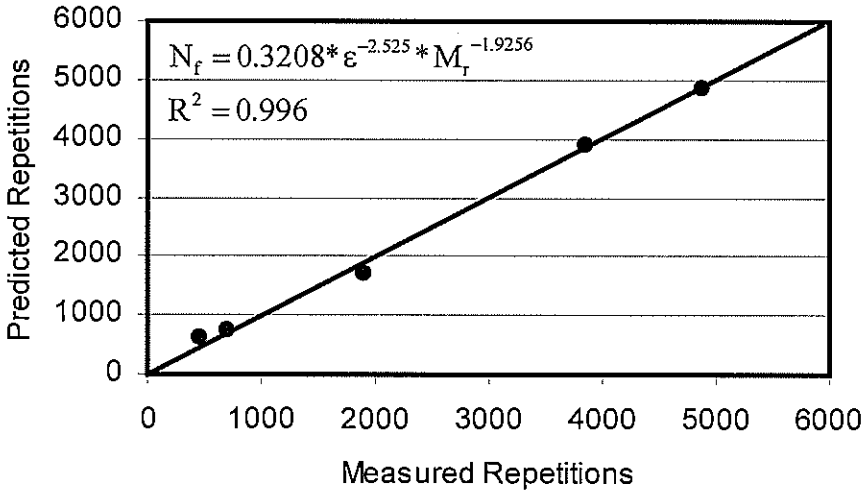

Figure 5.18 Predicted versus measured number of load repetitions for foam-stabilised mix using equation 16 model.

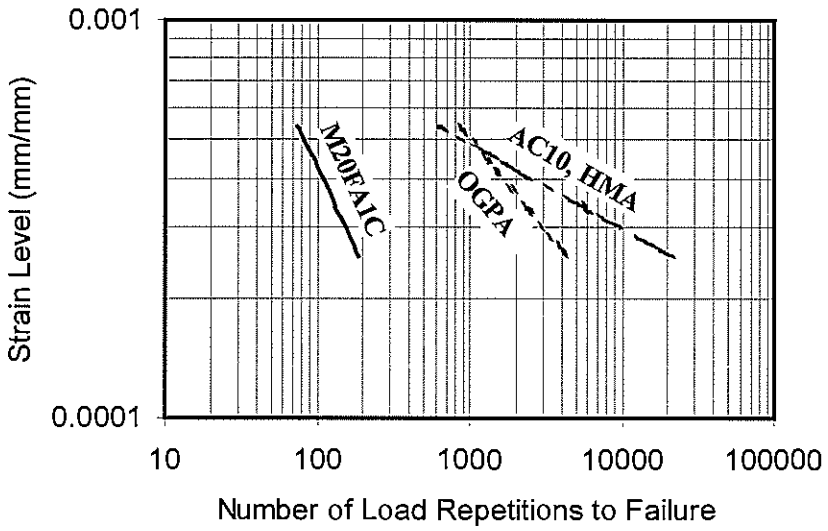

Figure 5.19 Fatigue life for the 3 different types of mixes M20FA1C, OGPA, and AC10 HMA.

5.8 California Bearing Ratio (CBR)

Four different types of mixes were prepared using AP-40 and AP-20 aggregate gradations with lime (LM) and Huntly pond ash (PA) as mineral fillers. Each CBR specimen was prepared in accordance with NZS 4407:1991 Test 3.15 and compacted in accordance with NZS 4402: Test 4.1.1. The four types of mixtures used in this investigation were M20LM, M20PA, M40LM, and M40PA. The mixtures were later cured for three days and soaked for four days. After that the Humboldt Master Loader HM-3000 (shown in Figure 5.7) was used to determine the CBR of the mixtures using a loading speed of 1 mm/min as specified in the standard.

Two unstabilised aggregates using the upper limit gradation of the conventional AP-40 and the mid-point gradation of the AP-20 were prepared and tested for CBR without curing or soaking. These results were then compared with the previous soaked CBR values of the four series.

Table 5.9 contains the CBR values for foam-stabilised mixes and those for conventional aggregates. Figure 5.20 shows the effects of aggregate gradation, type of mineral fillers, and foam stabilisation on the CBR values. For all the foam-stabilised mixes, the CBR values after 4 days of soaking are higher than the CBR values for the unsoaked conventional aggregates (Table 5.9). This proves that the moisture resistance of the foam-stabilised mixes is quite high, and mixes using Huntly pond ash showed higher CBR values than those using hydrated lime as mineral fillers.

Table 5.9 CBR values (%) for foam-stabilised mixes and conventional aggregates.

Type of Material	Soaked CBR	Unsoaked CBR
M20LM	110	
M20PA	225	
M40LM	135	
M40PA	260	
Aggregate AP-20 (Midpoint gradation)	–	87.5
Aggregate AP-40 (Upper limit gradation)	-	85

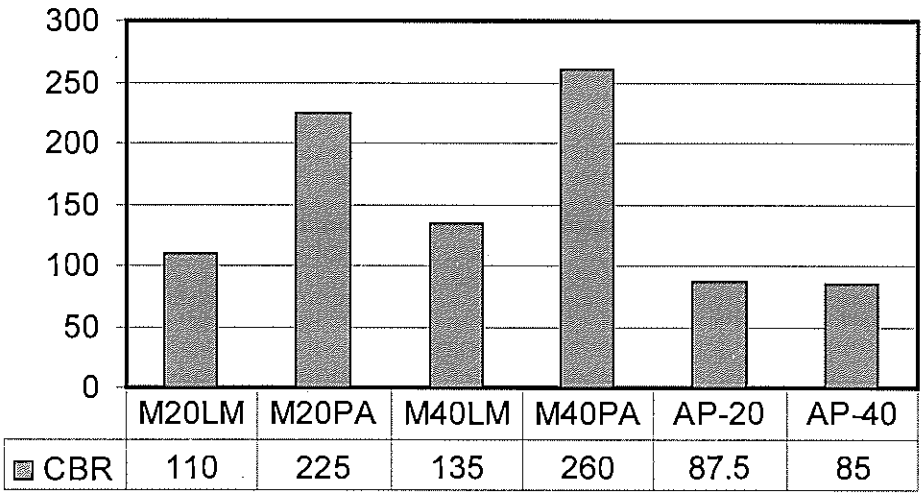

Figure 5.20 Comparison between the CBR values (%) for the foam-stabilised mixes and conventional aggregates.

6. Conclusions and Recommendations

The behaviour of the foamed-bitumen mixes produced from different bitumen types, using different aggregate gradations, and different types of mineral fillers, was conducted for the research recorded in this report.

Foaming Characterisation

The experimental work presented includes the foaming characterisation of bitumens from seven sources. According to the foam index parameter, VEN180 and AR4000-1 provided the best quality foam while C170, SHL80 and DLT80 resulted in a foamed bitumen of poorest quality. The current foamability test parameters showed discrepancies in characterising the foam quality of the different types due to the empirical nature of the test.

New Characterisation System

A new characterisation system based on the average viscosity of the foamed bitumen obtained over a period of 60 seconds has been introduced and examined for different bitumen types. Foam viscosity is a fundamental parameter, and it is unlikely to show inconsistencies in the results. Also the suggested new system provides a way to optimise the foamant water content, and also provides a direct measurement of the actual viscosity of the foam. It is unlike the empirical characterisation system used currently which is based on Expansion Ratio, Half-life Time, and Foam Index and does not give exact values for viscosity of the foam.

Volumetric Properties

Volumetric properties of the foam-stabilised mixes showed that the percentage of air voids in the total mix (VA%) was about twice that of the dense-graded HMA. However, the percentage of voids in the mineral aggregates (%VMA) of the foam-stabilised mixes was very close to that of HMA made with aggregates of the same maximum nominal size.

Temperature Susceptibility

The temperature susceptibilities of the different types of bitumen were investigated, as well as those of the mixes. Using bitumen that has low temperature susceptibility produced foamed-stabilised mixes that also had low temperature susceptibilities. However, some bitumens with high temperature susceptibilities produced foam-stabilised mixes with a moderate temperature susceptibility.

Comparing the temperature susceptibility of HMA with that of foam-stabilised mixes made with the same bitumen type showed that the HMA mixes are more sensitive to temperature variations. At temperatures about 30°C or higher, foam-stabilised mixes have higher resilient modulus values than those of HMA mixes. These higher values indicate that foam-stabilised mixes are likely to be more resistant to rutting than HMA at high temperatures.

The temperature susceptibility of New Zealand bitumen was found to be lower than those for the US and Australian sources used in this study.

Moisture Susceptibility

The moisture susceptibility of foam-stabilised mixes, especially the effect of bitumen source and grade on moisture susceptibility as shown by the Index of Retained Strength (IRS), was studied. While the bitumens from some sources provided higher values of IRS than bitumens from other sources, foam-stabilised mixes, in general, provided excellent moisture resistance as their IRS exceeded 80% – 90% after 5 days of soaking.

Indirect Tensile Strength

The indirect tensile strength test (ITS) was carried out for different foam-stabilised mixes and was compared with that for HMA. HMA provided higher ITS values compared to foam-stabilised mixes. The effects of gradation and the type of mineral fillers were quite noticeable, as active fillers such as fly ash type C and Portland cement noticeably improved the ITS values for foam-stabilised mixes.

Fracture Energy

The fracture energy of foam-stabilised mixes and AC10 HMA was investigated and, in addition, the effect of the rate of loading on the fracture energy. Again, HMA mixes provided the highest fracture energy compared to foam-stabilised mixes which confirms the high fatigue resistance of HMA. The effect of rate of loading on the fracture energy of the foam-stabilised mixes was large, which affirms that these mixes show viscoeleastic behaviour.

Fatigue Behaviour

The fatigue behaviour of the foam-stabilised mixes was investigated, as well as that of dense-graded AC10 HMA and open-graded porous asphalt (OGPA), to compare their fatigue life performance.

Foam-stabilised mixes provided a lower fatigue life compared to HMA and OGPA. However, if the bitumen and mineral filler contents were to be optimised so that the indirect tensile strength or fatigue energy were maximised, then the fatigue life of these mixes could be improved.

The fatigue models developed in this study should only be used for purposes of comparison. These fatigue models were developed using the indirect tensile fatigue test with constant stress mode and only one replicate for each stress level was made. In order to get more reliable fatigue models, with which to determine the actual fatigue life, a more comprehensive testing programme is required to use different test methods such as beam fatigue, and other modes of testing such as constant strain test.

In addition to the resilient modulus, some parameters such as indirect tensile strength or fracture energy are recommended for inclusion in the mix design procedure. The foam, water content, and the ratio between foam and mineral fillers content should be determined to optimise the value of ITS or fracture energy, to ensure longer fatigue life for these mixes.

CBR Values

The CBR test was conducted on foam-stabilised mixes having different gradations and mineral fillers, and compared with unstabilised aggregate complying with the midpoint of AP-20 and upper limit of the AP-40 gradations. The effect of foam stabilisation on CBR is quite obvious as the soaked CBR of the stabilised mixes exceeds the dry CBR of the unstabilised aggregates.

The type of mineral fillers played an important role on the effect on the CBR value. For example, mixes incorporating the Huntly pond ash fillers provided higher CBR values than mixes with hydrated lime.

Summary

The foam-stabilised mixes had reasonably good behavioural characteristics in the laboratory and they are expected to perform reasonably well in the field.

A more extensive testing programme is required to further investigate the fatigue behaviour of the different categories of the foam-stabilised mixes and a field calibration of the laboratory-developed models is required.

7. References

APRG. 2002. Australian Provisional Guide: Selection and design of asphalt mixes. *APRG Report No. 18.*

Bissada, A.F. 1987. Structural response of foamed asphalt sand mixtures in hot environments. *Transportation Research Record 1115:* 134-149. Washington DC, USA.

Jenkins, K.J., van de Ven, M.F.C., de Groot, J.L.A. 1999. Characterisation of foamed bitumen. *Proceedings 7th Conference on Asphalt Pavements for Southern Africa (CAPSA '99):* 1-18.

Lee, D.Y. 1981. Treating marginal aggregates and soils with foamed asphalt. *Proceedings of the Association of Asphalt Pavement Technologists 50:* 211-250.

Maccarrone, S., Holleran, G., Leonard, D.J., Dip, S.H. 1994. Pavement recycling using foamed bitumen. *Proceedings 17th Australian Road Research Board Conference, Part 3:* 349-365. ARRB Conference, Gold Coast, Queensland.

Mohammad, L.N., Abu-Farsakh, M.Y., Wu, Z., Abadie, C. 2003. Louisiana experience with foamed recycled asphalt pavement base materials. *Transportation Research Board TRR 1832:* 17-24.

Muthen, K.M. 1999. Foamed asphalt mixes – mix design and procedure. *CSIR Contract Report No. CR-98/077.* 39pp. CSIR Transportek, South Africa.

Ramanujam, J.M., Jones, J.D. 2000. Characterisation of foamed bitumen stabilization. *Proceedings Road System and Engineering Technology Forum:* 1-22. Queensland, Australia.

Read, J.M., Brown, S.F. 1966. Practical evaluation of fatigue strength for bituminous paving mixtures. *Proceedings Eurobitume/Eurasphalt Congress*, Strasbourg, 1996.

Read, J.M., Brown, S.F. 1996. Fatigue characterisation of bituminous mixes using a simplified test. Pp. 158-172 in *Proceedings of Symposium on Performance and Durability of Bituminous Materials* (Cabrera, J.G., Dixon, J.R. Editors). E & F N Spon, London.

Roberts, F.L., Kandhal, P.S., Brown, E.R., Lee, D.Y. 1991. *Hot mix asphalt materials, mixture design, and construction.* NAPA Educational Foundation, Lanham, Maryland, USA.

Roberts, H.S. 1996. *Writing for science: a practical handbook for science, engineering and technology students.* Longman, Auckland, New Zealand.

Saleh, M.F., Herrington, P. 2003. Foamed bitumen stabilisation for New Zealand roads. *Transfund New Zealand Research Report No. 250.* 88pp.

South Africa Transportek. 2002. The design and use of foamed bitumen treated materials. *South African Interim Technical Guidelines.* CSIR Transportek, South Africa.

Standards

AS/NZS 2891-1986 Methods of sampling and testing asphalt. Joint AS NZ Standard.

AS 2891.1-1986 Methods of sampling and testing asphalt. Method 1.1: Sampling of asphalt.

AS 2891.2.2-1986 Methods of sampling and testing asphalt. Method 2.2: Sample preparation – compaction of asphalt testing specimens using a gyratory compactor.

AS 2891.8-1993 Methods of sampling and testing asphalt – Voids and density relationships for compacted asphalt mixes.

AS 2891.13.1-1995 Methods of sampling and testing asphalt. Method 13.1: Determination of the resilient modulus of asphalt – indirect tensile method.

ASTM C127-04 Standard test method for density, relative density (specific gravity), and absorption of coarse aggregates.

ASTM C128-04 Standard test method for density, relative density (specific gravity), and absorption of fine aggregates.

ASTM D5-97 Standard test method for penetration of bituminous materials.

ASTM D36-95 Standard test method for softening point of bitumen (Ring-and-Ball apparatus).

ASTM D1559-89. Standard test method for resistance to plastic flow of bituminous mixtures using Marshall apparatus.

ASTM D4402-02 Standard test method for viscosity determination of asphalt at elevated temperatures using a rotational viscometer.

ASTM D5581-96 (2001) Standard test method for resistance to plastic limit of bituminous mixtures using Marshall apparatus (6-inch diameter specimen).

NZS 3112: Part 2:1986 Methods of test for concrete. Tests relating to the determination of strength of concrete.

NZS 4402:1986 Methods of testing soils for civil engineering purposes.

NZS 4402: Part 4 Soil compaction tests, Section 4.1 Determination of the dry density/water content relationship. Test 4.1.1:1986 New Zealand standard compaction test.

NZS 4402: Part 4 Soils compaction tests. Section 4.1 Determination of the dry density/water content relationship. Test 4.1.3:1986 New Zealand vibrating hammer compaction test.

NZS 4407:1991 Methods of sampling and testing road aggregates. Part 3 Methods of testing road aggregates – laboratory tests. Test 3.15 The California Bearing Ratio (CBR).